Electronic Supplementary Material (ESI) for Inorganic Chemistry Frontiers.

Supporting Information

Acid-induced Conversion of Nitrite to Nitric Oxide at Copper(II) Center: A New Catalytic Pathway

Prabhakar Bhardwaj,[a] Kulbir,[a] Tarali Devi,*[b] Pankaj Kumar*[a]

[a]Department of Chemistry, Indian Institute of Science Education and Research (IISER), Tirupati 517507, India

[b]Department of Inorganic and Physical Chemistry, Indian Institute of Science Bangalore 560012, India

* To whom correspondence should be addressed.

E-mail: pankaj@iisertirupati.ac.in

Table of Contents

Experimental Section

Experimental Section

Materials. All reagents and solvents obtained from commercial sources (Sigma Aldrich Chemical Co. and Tokyo Chemical Industry) were of the best available purity and were used without further purification unless otherwise indicated. Solvents were dried according to reported literature and distilled under an inert atmosphere before use.[S1] $Na^{15}NO_2$ (99.2% ^{15}N-enriched) was purchased from ICON Services Inc. (Summit, NJ, USA). $Na^{18}ONO$ (99% ^{18}O-enriched) was purchased from ICON Services Inc. (Summit, NJ, USA). The 12-TMC ligand was prepared by reacting excess amounts of formaldehyde and formic acid with 1,4,7,10-tetraazacyclododecane as reported previously.[S2]

Instrumentation. UV-Vis spectra were recorded on an Agilent tec Cary 8454 diode array spectrometer equipped with a thermostat cell holder (UNISOKU Scientific Instruments) designed for low-temperature experiments. FT-IR spectra in solid form were recorded on Bruker-Alpha Eco-ATR FTIR spectrometer using the standard KBr disk method. The FT-IR spectra were recorded on the Bruker-Alpha Eco-ATR FTIR spectrometer using the KBr disk method. ^{1}H-NMR spectra were measured with a Bruker model Ascend 400 FT-NMR spectrometer. Electrospray ionization mass spectra (ESI-MS) were recorded on an Agilent Mass Spectrometer (6200 series TOF/6500 series Q-TOF B.08.00) by infusing samples directly into the source using a manual method. The spray voltage was set at 4.2 kV, and the capillary temperature was at 80 °C. GC-MS analyses were recorded on an Agilent 7890B GC system equipped with a 5977B MSD Mass analyzer. Single crystal X-ray diffraction data were collected using Bruker D8 Venture super Duo diffractometer with Photon-III detector using Mo source(λ = 0.71073 Å).

Synthesis of [(Me_2BPMEN)$Cu^{II}(ClO_4)$](ClO_4) (3). A CH_3CN solution (5 mL) of Copper(II) perchlorate hexahydrate (370.54 mg, 1.0 mmol) was added to a 20 ml CH_3CN solution of Me_2BPMEN (270.18 mg, 1.0 mmol) with constant stirring for 1 hour at RT (298

K). The color of the solution appeared blue instantly with the addition of Copper(II) perchlorate hexahydrate from yellow. After the completion of the reaction, the volume of the reaction mixture was reduced under reduced pressure, and diethyl ether was added to precipitate complex **3** (blue color). Yield: 480 mg (~ 90%). UV: λ_{max} = 620 nm (ε = 230 M^{-1} cm^{-1}). FT-IR (KBr pellet): 2930, 1609, 1450, 1100 cm^{-1}. Mass (*m/z*): Calcd*:* 333.1, Found: 333.1. Anal. Calcd. For $C_{16}H_{22}Cl_2CuN_4O_8$: C, 36.07; H, 4.16; N, 10.52; Found : C, 36.18; H, 4.13; N, 10.45.

Synthesis of [(Me_2BPMEN)$Cu^{II}(NO_2^-)$](ClO_4) (1). To a 20 ml CH_3CN solution of [(Me_2BPMEN)$Cu^{II}(ClO_4)$](ClO_4) (532.8 mg, 1.0 mmol), 1.0 mL aqueous solution of $NaNO_2$ (69 mg, 1.0 mmol) was added slowly with constant stirring and the color of the reaction mixture changes from blue to cyan-green. The mixture was stirred for 1 hour at 298 K. The volume of the reaction mixture was decreased to 10 mL under reduced pressure and then layered with diethyl ether and kept for crystallization at 298 K. Yield: 440 mg (~ 95 %). UV: λ_{max} = 375 nm (ε = 780 M^{-1} cm^{-1}). FT-IR (KBr pellet): 2930, 1442, 1604, 1270, 1100 cm^{-1}. Mass (*m/z*): Calcd: 379.1, Found: 379.1. Anal. Calcd. For $C_{16}H_{22}ClCuN_5O_6$: C, 40.09; H, 4.63; N, 14.61; Found : C, 40.15; H, 4.55; N, 14.58

Synthesis of [(Me_2BPMEN)$Cu^{II}(^{15}NO_2^-)$](ClO_4) (1-$^{15}NO_2^-$). To a 20 ml CH_3CN solution of [(Me_2BPMEN)$Cu^{II}(NCCH_3)$](ClO_4)$_2$ (53.2 mg, 0.1 mmol), 1.0 mL aqueous solution of $Na^{15}NO_2$ (7 mg, 0.1 mmol) was added slowly with constant stirring and the color of the reaction mixture changes from blue to cyan-green. The mixture was stirred for one hour at RT (298 K). The volume of the reaction mixture was decreased to 10 mL over a rotary vacuum and then layered with diethyl ether and kept for crystallization at 298 K. Yield: 43.7 mg (~ 91%). FT-IR (KBr pellet): 2930, 1445, 1605, 1244, 1100 cm^{-1}. Mass (*m/z*): Calcd: 380.1, Found: 380.1. [(Me_2BPMEN)$Cu^{II}(^{18}ONO^-)$](ClO_4) (**1-$^{18}ONO^-$**) complex was prepared following the same method by using an ^{18}O-labelled $Na^{18}ONO$. FT-IR (KBr pellet): 1243, 1100 cm^{-1}.

Synthesis of [(H_2BPMEN)Cu^{II}](ClO_4)$_2$ (4). A CH_3CN solution (5.0 mL) of Copper(II) perchlorate hexahydrate (370.54 mg, 1.0 mmol) was added to a 20 ml CH_3CN solution of H_2BPMEN (242.15 mg, 1.0 mmol) with constant stirring for one hour 298 K. The color of the solution appeared blue instantly from yellow with the addition of Copper(II) perchlorate hexahydrate. After the completion of the reaction, the volume of the reaction mixture was reduced through a rotary vacuum, and diethyl ether was added to precipitate complex **4** (blue color). Yield: 454.28 mg (~ 90 %). UV: λ_{max} = 600 nm (ε = 220 M^{-1} cm^{-1}). FT-IR (KBr pellet): 3245, 1615, 1434, 1100 cm^{-1}. Mass (*m/z*): Calcd: 152.5, Found: 152.5. Anal. Calcd. For $C_{14}H_{18}Cl_2CuN_4O_8$: C, 33.31; H, 3.59; N, 11.10; Found : C, 33.25; H, 5.45; N, 11.15.

Synthesis of [(H_2BPMEN)Cu^{II}(NO_2^-)](ClO_4) (2). To a 20 ml CH_3CN solution of [(H_2BPMEN)Cu^{II}($NCCH_3$)](ClO_4)$_2$ (532.82 mg, 1.0 mmol), 1.0 mL aqueous solution of $NaNO_2$ (69 mg, 1.0 mmol) was added slowly with constant stirring and the color of the reaction mixture changes from blue to cyan-green. The mixture was stirred for one hour at RT (298 K). The volume of the reaction mixture was decreased to 10 mL over a rotary vacuum, and then complex **2** was isolated as a deep blue color precipitate compound with diethyl ether. Yield: 406.17 mg (~ 90 %). UV: λ_{max} = 360 nm (ε = 700 M^{-1} cm^{-1}). FT-IR (KBr pellet): 3149, 1600, 1397, 1270, 1100 cm^{-1}. Mass (*m/z*): Calcd: 351.1, Found: 351.1. Anal. Calcd. For $C_{14}H_{18}ClCuN_5O_6$: C, 37.26; H, 4.02; N, 15.52; Found : C, 37.28; H, 4.06; N, 15.46.

Synthesis of [(H_2BPMEN)Cu^{II}($^{15}NO_2^-$)](ClO_4) (2-$^{15}NO_2^-$). To a 20 ml CH_3CN solution of [(H_2BPMEN)Cu^{II}](ClO_4)$_2$ (53.2 mg, 0.1 mmol), 1.0 mL aqueous solution of $Na^{15}NO_2$ (7 mg, 0.1 mmol) was added slowly with constant stirring and the color of the reaction mixture changes from blue to cyan-green. The mixture was stirred for one hour at RT (298 K). The volume of the reaction mixture was decreased to 10 mL over a rotary vacuum, and then Diethyl ether was added to precipitate the complex **2**-$^{15}NO_2^-$. Yield: 40.7 mg (~ 90 %). FT-IR (KBr pellet): 2909, 1612, 1370, 1244, 1100 cm^{-1}. Mass (*m/z*): Calcd: 352.1, Found: 352.1.

Reaction of [(Me_2BPMEN)$Cu^{II}(NO_2^-)$](ClO_4) (1) + one equiv Acid ($HClO_4$, H^+). Complex **1** was reacted with the equimolar amount of perchloric acid ($HClO_4$) in CH_3CN under Argon atmosphere at RT. The color of the above reaction mixture changed from cyan-green to blue upon adding one equiv H^+, indicating the formation of **3**. The product obtained in the reaction of **1** and one equiv H^+ was compound **3** and confirmed with the help of various spectroscopic and structural characterizations. UV: λ_{max}(CH_3CN) = 620 nm (ε = 230 M^{-1} cm^{-1}). FT-IR (KBr pellet): 2930, 1609, 1450, 1100 cm^{-1}. Mass (*m/z*): Calcd*:* 333.1, Found: 333.1.

Reaction of [(H_2BPMEN)$Cu^{II}(NO_2^-)$](ClO_4) (2) + one equiv Acid ($HClO_4$, H^+). Complex **2** was reacted with the equimolar amount of perchloric acid ($HClO_4$) in CH_3CN under Argon atmosphere at RT. The color of the above reaction mixture changed from cyan-green to blue upon adding one equiv H^+, indicating the formation of **4**. The product obtained in the reaction of **2** and H^+ was confirmed to be compound **4** from various spectroscopic and structural characterizations. UV: λ_{max} = 600 nm (ε = 220 M^{-1} cm^{-1}). FT-IR (KBr pellet): 3245, 1615, 1434, 1100 cm^{-1}. Mass (*m/z*): Calcd*:* 152.5, Found: 152.5.

Trapping of $NO_{(g)}$ with [(12-TMC)Co^{II}](BF_4)$_2$. [(12-TMC)Co^{II}] (BF_4)$_2$ (0.461 g, 1.0 mmol) was used for the quantitative trapping of $NO_{(g)}$. A small culture vial with the solution of **1** (40 mM) in Argon-saturated CH_3CN was placed in a larger vial containing a solution of [(12-TMC)Co^{II}](BF_4)$_2$ (40 mM) in Argon-saturated CH_3CN. The larger vial was sealed with the septum. A solution of $HClO_4$ (one-equiv, 40 mM) in Argon-saturated CH_3CN was injected into the inner vial, the solution was stirred for 3 hours, and the complete setup was left at 273 K overnight. Then the product was precipitated out by using diethyl ether. Further, the product was characterized by using various spectroscopic methods. The UV-Vis spectrum of the product (λ_{max} = 370 nm) was compared with the authentic sample (λ_{max} = 370 nm), which confirms the formation of [(12-TMC)Co^{III}(NO)](BF_4)$_2$ and quantifies the yield of $\{CoNO\}^8$ around 90%. We observed the of formation of $\{CoNO\}^8$ around 85% when we reacted **1** with

2 equiv of H^+. Similar experiments were performed to trap the NO from **2** with one equiv of H^+ and one equiv of [(12-TMC)Co^{II}]$(BF_4)_2$. λ_{max} = 370 nm (ε = 800 M^{-1} cm^{-1}). FT-IR (KBr pellet): 2925, 1704, 1467, 1081 cm^{-1}. Mass (*m/z*): Calcd: 404.2, Found: 404.2 ([(12-TMC)Co^{III}(NO)(BF_4)]$^+$).

Reactivity studies. All UV-Vis spectral measurements were run in a UV cuvette in CH_3CN under Ar at RT. All kinetic reactions were run at least three times, and the data reported here are the average outcome for these reactions. We have performed all the reactions in the degassed solutions under Ar to avoid the interaction/reaction of dioxygen with nitrosyl /or nitric oxide (NO). The formation of {CoNO}^{8} complex and H_2O_2 in the above NO_2^- reduction reactions were identified by comparing with authentic samples, and the product yields were determined by comparison against standard curves prepared with original samples.

^{15}N-labeling experiments (following the N-atom by FT-IR and ESI-MS measurements): We have recorded the IR spectra of the different complexes in their solid form as KBr pellet to follow the source of N-atom ($^{14/15}$N). The IR spectra of complexes **1** and **2** showed a NO_2^- characteristic peak at 1270 cm^{-1}, which shifted to 1244 cm^{-1} when prepared with ^{15}N-labeled nitrite ($^{15}NO_2^-$). The change in the IR stretching frequency of copper bound NO_2^- (Δ = 26 cm^{-1}) confirmed that an increase in the reduced mass of nitrogen atom (^{14}N to ^{15}N) is responsible for the decrease in the stretching frequency of the NO_2^- functional group. As the Cu-nitrosyl was not stable enough to isolate, hence to follow the $NO_{(g)}$ generated in the Cu-bound NO_2^- reduction reaction, we have used our previously reported Co-12TMC complex to trap $NO_{(g)}$ as cobalt-nitrosyl complex ({CoNO}^{8}).[s3] We observed similar spectral shift/changes as observed for Cu-$^{14/15}NO_2^-$ complexes when the IR spectra were recorded for trapped {CoNO}^{8} in the acid-induced NO_2^--reduction (^{14}N and ^{15}N-labeled NO_2^-) in complexes **1** and **2**. The IR spectra of {CoNO}^{8} showed a characteristic nitrosyl stretching frequency at 1704 cm^{-1} (^{14}N), which shifted to 1674 cm^{-1} (Δ = 30 cm^{-1}) when exchanged with the ^{15}N-labeled nitrosyl functional

group. The ESI-MS spectra show a peak at 404.2 corresponds to $[Co(12TMC)(NO)(BF_4)]^+$ and shifted to 405.2, which corresponds to $[Co(12TMC)(^{15}NO)(BF_4)]^+$.

Qualitative and quantitative estimation of H_2O_2 by ^{1}H-NMR: To confirm the H_2O_2 formation in the reaction of **1** with one equiv $HClO_4$, we have monitored the one equiv acid-induced Cu-bound NO_2^--reduction reaction by ^{1}H-NMR spectroscopy. In this regard, the ^{1}H-NMR spectrum of complex **1** (9.56 mg / 500 μL, 40 mM) with one equiv $HClO_4$ in CD_3CN showed a signal at 8.66 ppm, which corresponds to H_2O_2., We compared the ^{1}H-NMR spectrum of the H_2O_2 formed in the above reaction with the authentic samples, H_2O_2 only (8.66 ppm) and H_2O_2 + **1** (8.66 ppm), which confirmed the formation of H_2O_2 and also validated our hypothesis of H_2O_2 formation in the NO_2^- reduction chemistry. Additionally, we have calculated the amount of H_2O_2 generation by comparing peak-integral corresponding to H_2O_2 (8.66 ppm) of the reaction mixture (**1** + $HClO_4$) with the authentic sample (20 mM H_2O_2 + **3**) containing an internal standard Benzene (8.66 ppm). The same reaction was performed using $DClO_4$; however, we did not observe any peak for hydrogen peroxide due to the formation of D_2O_2 in NMR. Note: All NMR spectra were recorded just after adding acid. Keeping the sample for a long showed the decomposition of the H_2O_2, so we did not get a 100 % yield of H_2O_2.

S. No.	Sample	The integral of benzene peak (7.37 ppm) (A)	The integral of the H_2O_2 peak (8.66 ppm) (B)	Ratio (B) / (A)
1	20 mM H_2O_2 + **3**	6	2.0	0.33
2	**2** + one equiv H^+	6	1.21	0.201
3	**2** + one equiv H^+	6	1.25	0.208
4	**2** + one equiv H^+	6	1.18	0.196

Amount of H_2O_2 formed:

Sample 1 = (0.201 / 0.33) × 20 mM =12.5 mM (31.25 %)

Sample 2 = (0.208 / 0.33) × 20 mM =12.6 mM (31.50 %)

Sample 3 = (0.196 / 0.33) × 20 mM =11.8 mM (29.65 %)

H_2O_2 formed in the reaction (average): = ~ 30.75 %

Estimation of H_2O_2 (*Iodometric-titration*): Additionally, the amount of H_2O_2 was determined by Iodometric-titration. We have titrated the amount of H_2O_2 generated in the 1 (0.1 mM) reaction with one equiv of perchloric acid (0.1 mM) in 2.5 mL CH_3CN under an argon atmosphere at 298K. The reaction solution was treated with an excess of sodium iodide (1.5 mM) under an argon atmosphere, and the UV-Vis spectrum was recorded for the reaction. As explained below, the quantity of I_3^- formed in the reaction was determined at 361 nm due to I_3^- (λ max 361 nm, $\varepsilon = 2.8 \times 104\ M^{-1}\ cm^{-1}$).

Amount of H_2O_2 formed:

Sample 1 = (Abs. = 0.87) = 0.031 mM (~ 31 % of H_2O_2)

Sample 2 = (Abs. = 0.90) = 0.032 mM (~ 32 % of H_2O_2)

Sample 3 = (Abs. = 0.85) = 0.030 mM (~ 30% of H_2O_2)

H_2O_2 formed in the reaction (average): = ~ 31 %

Also, H_2O_2 formed in complex **2** (0.1 mM) reaction with two equiv of perchloric acid (0.2 mM) was determined under similar conditions. The reaction solution was treated with an excess of sodium iodide (2 mM) in CH_3CN under an argon atmosphere, and the UV-Vis spectrum was recorded for the reaction (Figure S13b). No I_3^- formation was observed in this reaction mixture.

Confirming the formation of proposed Cu^{II}(ONOH) intermediate (•OH radical trapping experiment): To confirm the N–O bond homolysis and the formation of free •OH radical, we have performed the •OH radical trapping experiment using 2,4-di-tert-butyl-phenol

(2,4-DTBP). For this reaction, we have reacted complex **1** (1.0 mM) with 2,4-DTBP (2.5 mM) in the presence of one equiv perchloric acid in acetonitrile at RT under Ar. The reaction mixture was then analyzed using GC-MS for identification, and LC quantified the amounts of reaction products against the standard plots of all the compounds. In this experiment, we observed the formation of 3,5-Di-tert-butyl catechol (3,5-DTBC) with small amounts of 2,4-DTBP-dimer (3,5-DTBP-D) and nitro-2,4-DTBP (nitro-3,5-DTBP), suggesting the N–O bond homolysis to form free •OH radical and hence indirectly proving the Cu-nitrousacid intermediate. The amount of 3,5-DTBC formed in the reaction was found to be ~ 20 % (0.20 mM), accounting for 40 % •OH radical, 2,4-DTBP-D (~ 10 %, 0.05 mM, 20 % •OH radical), and nitro-2,4-DTBP (~ 4 %, 0.013 mM, 12 % •OH radical) in the reaction mixture, because a specific amount of •OH decomposes to other side products due to its high reactivity. Additionally, we prepared **1**-$^{18}ONO^-$ to generate [Cu-$^{16}O^{14}N^{18}OH]^{2+}$ intermediate species and trapped it using the 2,4-DTBP test. In the reaction mixture, we observed the formation of 3,5-DTBC(^{18}OH) and 3,5-DTBC(^{16}OH), with the formation of $^{16}O^{14}N^{18}O$-DTBP.

Trapping of H_2O_2 using thioanisole: We performed the H_2O_2 trapping experiment using thioanisole to confirm the formation of H_2O_2 in the acid-induced NO_2^- reduction. For this reaction, we have reacted **2** (1.0 mM) with one-equiv of H^+ in CH_3CN at 293 K under Ar atmosphere; and the reaction was monitored using UV-Vis spectroscopy. After completion of the reaction, 0.5 mM solution of thioanisole in CH_3CN was added to the reaction mixture, and the qualitative analysis of the reaction mixture was performed using GC-MS showing the formation of methyl phenyl sulfoxide and hence indirectly proving the presence of H_2O_2 in the reaction mixture.

Time-dependent detection of NO gas using headspace gas mass spectrometry: We detected the $NO_{(g)}$ ($^{14}NO/^{15}NO$) formed in the reaction of **1** and **2** with acid ($HClO_4$) using an online MS with an OmniStar^{TM} Gas Analysis System GSD 320 (Pfeiffer) quadrupole mass

spectrometer apparatus. In order to follow the $NO_{(g)}$ generated in the NO_2^- reduction, two sample vials (5.0 mL) containing a CH_3CN solution of **1** and **2** (5.0 mM, 2.0 mL) sealed with a rubber septum were taken from the glove box and attached to the capillary from mass spectrometry into the headspace of the sealed vial for real-time measurement. $HClO_4$ (10 mM) solution was prepared in CH_3CN in other sample vials inside the glove box. One equiv amount of $HClO_4$ (100 µl, 10 mM) was added to the solution of **1** and **2** using a gas-tight Hamilton syringe, piercing through the rubber septum. The reactions were kept for 10 minutes at RT (298 K) before analyzing the target gases ($^{14}NO/^{15}NO$). We observed the formation of ^{14}NO and ^{15}NO gases. A similar process was followed to see the $^{14}NO/^{15}NO$ gas generation on reaction with **1** and **2** with two equiv of $HClO_4$ (100 µl, 20 mM). The detection of $N^{18}O$ and $N^{16}O$ was carried out following the above-demonstrated procedure for the reaction of **1**-$^{18}ONO^-$ with $HClO_4$.

Calculation of Binding Constant (K_b): The binding constants, **1**-K_b, and **2**-K_b, were determined by titrating complexes **3** and **4** for the different concentrations of NO_2^- respectively. The stock solutions of **3** and **4** (1 mM) were prepared in CH_3CN, and the guest molecules (Na NO_2, 1.0 mM) solution was prepared using crown ether in CH_3CN. Solutions of complexes **3** and **4** were prepared separately with increasing concentrations of the guest molecules. The UV-Vis spectra of these solutions were recorded to get absorbance values. The binding constants were calculated using the Benesi-Hildebrand equation.[S4-S5] K_b was calculated from the below equation.

$$1/(A\text{-}A_o) = 1/\{K_b(A_{max}–A_o)\,[X]_n\} + 1/[A_{max}\text{-}A_o]$$

Here, A_o is the absorbance of **3** and **4** in the absence of guests, A is the absorbance in the presence of guests at different concentrations, and A_{max} is the absorbance in the presence of added $[X]_{max}$ where X was NO_2^-, respectively. K_b is the binding constant (M^{-1}). The binding constants (K_b) were determined from the slope of the straight line of the plot of 1/(A-Ao)

against $1/(Amax–Ao)[X]_n$. The binding constants (K_b) as determined by the UV-Vis titration method for **1** and **2**, with NO_2^- are found to be 8.3×10^2 M^{-1} & 1.56×10^3 M^{-1} for **1** and **2**, respectively

Catalytic reactivity of complex 1 with excess H^+ and $NaNO_2$. To check the catalytic reactivity of **1,** we reacted **1** with H^+, followed by $NaNO_2$, and then again with H^+. 100mg (0.20 mmol) of complex **1** was dissolved in 2 mL of dry CH_3CN in a 10 mL vial, sealed with an airtight rubber septum inside the glovebox, and taken out. A standard UV spectrum of 1 mM complex **1** in CH_3CN at 298 K was recorded. One equiv of $HClO_4$ dissolved in CH_3CN was purged with Argon for 15 minutes and then added to the solution of **1** under Ar at 298 K. Addition of acid immediately changed the color from cyan green to blue, and the reaction was stirred for further 15 minutes. After 15 minutes, the solution was frozen and vacuum followed by purged with Ar using a standard Schlenk line to remove the $NO_{(g)}$ formed in the reaction. Then the standard spectra of the compound were taken, which matched the isolated complex **3**. Again, to the blue color solution of **3** formed in the above reaction, one equiv of $NaNO_2$ was added under Ar at 298 K. The color of the solution immediately changed from blue to cyan green indicating the conversion of **3** to **1**. The mixture was further stirred for 15 minutes, and standard UV-Vis spectra were taken after minutes, which matched the isolated complex **1**. The cyan-green solution was then purged with Ar and vacuum using a Schlenk line to remove any oxygen in the reaction system. One equiv of $HClO_4$ was added to the mixture under Ar at 298 K, immediately turning the solution color from cyan-green to blue. The solution was stirred for 15 minutes and, after 15 minutes, purged with Ar and vacuum. Then again, one equiv $NaNO_2$ was added under Ar at 298 K. The process was repeated for ten cycles, and a standard UV of **3** formed after 10 cycles were taken. Then again, $NaNO_2$ was added under Ar at 298 K to generate **1**. The standard UV of **1** was recorded in CH_3CN at 298 K, and the cycle was further repeated for another ten cycles. After ten cycles, the standard UV-Vis of **3** was recorded in

CH_3CN at 298 K. We determined the yield of complex **1** after ten cycles. The quantity of **1** generated after 10 cycles of catalytic reduction was determined at 375 nm (at λ_{max} 375 nm, ε = 780 M^{-1} cm^{-1}) as explained below.

S. No.	Sample (A)	Absorbance (B) (at 375 nm)	% Yield (C) (with respect to authentic sample)	% Yield C ×100
1	Authentic **1**	0.78		100
2	**1** generated after 2nd cycle	0.77	0.77/ 0.78 = 0.98	98
3	**1** generated after 4th cycle	0.76	0.76/ 0.78 = 0.97	97
4	**1** generated after 6th cycle	0.74	0.74/ 0.78 = 0.95	95
5	**1** generated after 8th cycle	0.72	0.72/ 0.78 = 0.92	92
6	**1** generated after 10th cycle	0.71	0.71/ 0.78 = 0.91	91

Average amount of **1** formed after Ten cycles of catalysis **= ~ 95 %**

Single-Crystal XRD Studies. Crystals were mounted on Hampton cryo-loops. All geometric and intensity data for the crystals were collected using a Bruker D8 Venture super Duo diffractometer with Photon-III detector using a Mo source diffractometer equipped with a micro-focus sealed X-ray tube Mo-Kα (λ = 0.71073 Å) X-ray source and HyPix3000 (CCD plate) detector of with increasing ω (width of 0.3 per frame) at a scan speed of either 5 or 10 s/frame. The CrysAlisPro software was used for data acquisition and data extraction. Using Olex2[S6], the structure was solved with the SIR2004[S7] structure solution program using Direct Methods and refined with the ShelXL[S8] refinement package using Least Squares minimization. All non-hydrogen atoms were refined with anisotropic thermal parameters. Detailed crystallographic data and structural refinement parameters are summarized in Table T1 - T4. CCDC 2176961 (**1**), and 2176962 (**3**) contain the supplementary crystallographic data for this

paper. These data can be obtained free of charge from The Cambridge Crystallographic Data Centre.

Nitric Oxide Preparation and Purification. NO was prepared and purified by following a detailed procedure, as shown in Figure S21. First, $NO_{(g)}$ was prepared by reacting $NaNO_2$ with H_2SO_4 under an Ar atmosphere and then passed through two different types of columns. First, pass through a column filled with NaOH beads to remove higher nitrogen oxide impurities. After that, the gas passes through two columns filled with NaOH beads molecular sieves to remove the minor amount of higher nitrogen oxides and moisture impurities. The highly purified $NO_{(g)}$ was then collected in a vacuum Schlenk flask fitted with a rubber septum (free from oxygen; after several vacuum and Ar purging). High-pressure $NO_{(g)}$ (with pressure >1 atmosphere; the septum bulges outward due to high pressures) then passes through an Ar-saturated (oxygen-free) and dry Acetonitrile (CH_3CN) solution for 15 minutes. The concentration of NO in the NO-saturated CH_3CN solution is ~14 mM.[S9]

References

S1. Armarego, W. L. F.; Chai, C. L. L. *Purification of Laboratory Chemicals*, 6th ed.; Pergamon Press: Oxford, **2009**.

S2. Halfen, J. A.; Young, V. G., Jr. Efficient Preparation of 1,4,8-trimethyl cyclam and its Conversion into a Thioalkyl-pendant Pentadentate Chelate. *Chem. Commun*. **2003**, 2894.

S3. Kumar, P.; Lee, Y. M.; Park, Y. J.; Siegler, M. A.; Karlin, K. D.; Nam, W., Reactions of Co(III)-nitrosyl complexes with superoxide and their mechanistic insights. *J Am Chem Soc*, **2015**, 137, 4284-4287.

S4. S. Goswami, D. Sen, N. K. Das, H. K. Fun, C. K. Quah, *Chem Commun (Camb)*, **2011**, *47*, 9101-9103.

S5. J. Chen, H. Yoon, Y. M. Lee, M. S. Seo, R. Sarangi, S. Fukuzumi, W. Nam, *Chem Sci*, **2015**, *6*, 3624-3632;

S6. Dolomanov, O. V.; Bourhis, L. J.; Gildea, R. J.; Howard, J. A. K.; Puschmann, H. OLEX2: a Complete Structure Solution, Refinement and Analysis Program. *J. Appl. Cryst*. **2009**, *42*, 339–341.

S7. Burla, M. C.; Caliandro, R.; Camalli, M. C., B.; Cascarano, G. L.; De Caro, L.; Giacovazzo, C.; Polidori, G.; Siliqi, D.; Spagna, R. IL MILIONE: A Suite of Computer Programs for Crystal Structure Solution of Proteins. *J. Appl. Cryst.* **2007**, *40*, 609–613.

S8. G. M. Sheldrick. Crystal Structure Refinement with SHELXL. *Acta Cryst*. **2015**, *C71*, 3–8.

S9. Young, C. L. *Solubility Data Series Val. 8 Oxides of Nitrogen,* International Union of Pure and Applied Chemistry (IUPAC), **1981**.

Table T1 Crystallographic data for **1** and **3**.

	1	**3**
Chemical formula	$C_{16}H_{22}ClCuN_5O_6$	$C_{16}H_{22}Cl_2CuN_4O_8$
Formula weight	479.37	532.82
Wavelength /Å	0.71073	0.71073
Crystal system	triclinic	triclinic
Space group	*P*-1	*P*-1
T, K	187(50)	100(2)
a, Å	7.4299(3)	8.8865(3)
b, Å	10.3318(3)	12.6743(4)
c, Å	13.5636(3)	18.5078(6)
α, °	77.258(2)	85.0760(10)
β, °	86.593(3)	84.0030(10)
γ, °	81.310(3)	84.6500(10)
V/ $Å^3$	1003.53(5)	2057.99(12)
Z	2	19
Calculated density, g/cm^3	1.586	1.720
Abs. Coeff. $/mm^{-1}$	1.265	1.375
Reflections collected	12147	144169
Unique reflections	4202	10238
Refinement method	Least-squares on F^2	Least-squares on F^2
Data/restraints/parameters	4202/0/273	10238/212/609
Goodness-of-fit on F^2	1.103	1.183
Final *R* indices [$I > 2\sigma(I)$]	R1 = 0.0504	R1 = 0.0315
	wR2 = 0.1360	wR2 = 0.0935
R indices (all data)	R1 = 0.0604	R1 = 0.0406
	wR2 = 0.1432	wR2 = 0.1103

Table T2 Selected bond lengths (Å) and bond angles (°) for **1** and **3**.

1		**3**	
Cu1 O1	1.996(2)	Cu1 N1	1.9993(17)
Cu1 N1	1.990(3)	Cu1 N2	2.0266(17)
Cu1 N2	2.038(3)	Cu1 N3	1.9894(16)
Cu1 N3	2.050 (3)	Cu1 N4	2.0231(17)
Cu1 N4	2.194(3)	Cu1 O1	2.2499(15)
O1 N5	1.289(4)		
O2 N5	1.230(4)		
Cu1 O2	2.650(2)		
N1 Cu1 O1	94.55(11)	N1 Cu1 N2	83.12(7)
N1 Cu1 N2	81.37(12)	N1 Cu1 N4	146.61(7)
N1 Cu1 N3	165.89(12)	N1 Cu1 O1	111.49(6)
N1 Cu1 N4	108.07(12)	N2 Cu1 N4	86.95(7)
N2 Cu1 O1	164.23(11)	N2 Cu1 O1	96.44 (6)
N3 Cu1 O1	92.32(11)	N3 Cu1 N1	102.46(7)
N4 Cu1 O1	95.49(11)	N3 Cu1 N2	167.87(7)
N2 Cu1 N4	103.43(11)	N3 Cu1 N4	82.53(7)
N2 Cu1 N3	86.37(12)	N3 Cu1 O1	91.53(6)
O2 N5 O1	114.2(3)	N4 Cu1 O1	101.24(6)

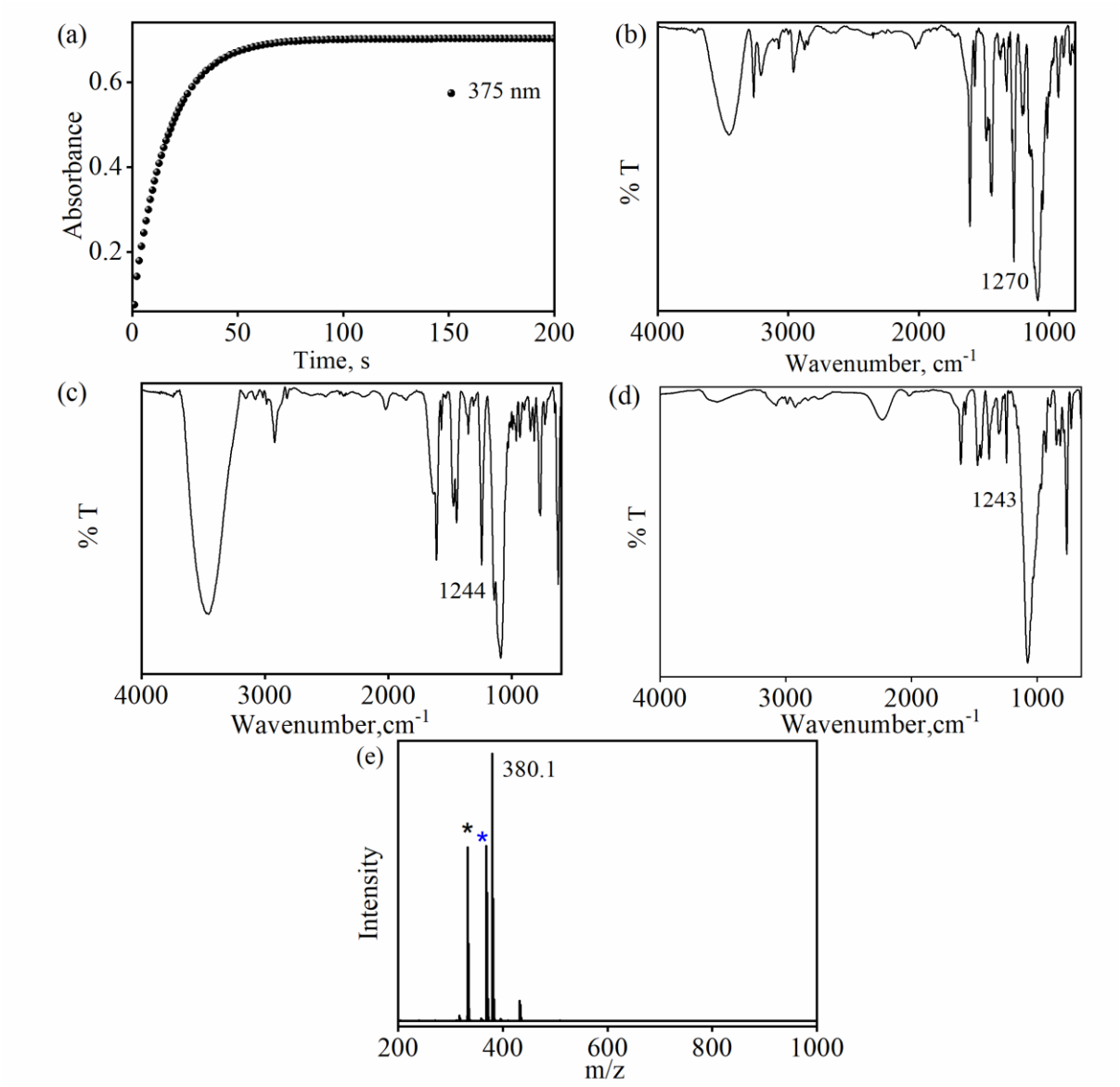

Figure S1. (a) Time course for the formation of **1** monitored at 375 nm upon addition of $NaNO_2$ (one equiv) to a solution of **3** (1 mM) in CH_3CN at 298 K. (b) FT-IR spectrum of **1** recorded in KBr pellet at 298 K, showing the peaks for **1**-$^{14}N^{16}O_2^-$ (1270 cm^{-1}). (c) FT-IR spectra of **1**-$^{15}N^{16}O_2^-$ (1244 cm^{-1}) recorded in KBr pellet at 298 K. (d) FT-IR spectrum of **1**-$^{18}ONO^-$ (1243 cm^{-1}) recorded in KBr pellet at 298 K. (e) ESI-MS spectrum of **1** recorded in CH_3CN. The peaks at *m/z* *333.1, *368.1 and 380.1 are assigned to be $[(Me_2BPMEN)Cu^{I}]^+$ (calcd: *m/z* 333.1), $[(Me_2BPMEN)Cu^{II}Cl]^+$ (calcd: *m/z* 368.1), $[(Me_2BPMEN)Cu^{II}(^{15}NO_2^-)]^+$ (calcd: *m/z* 380.1), respectively.

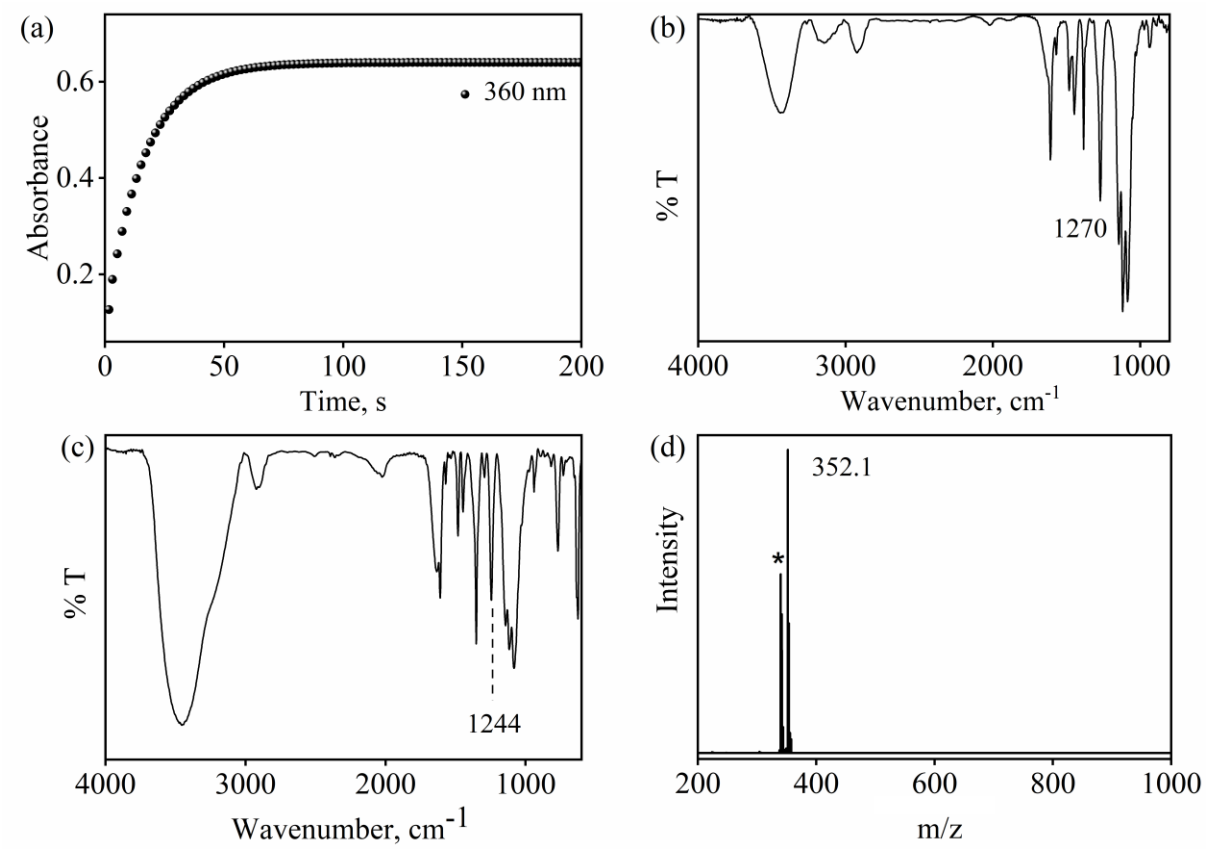

Figure S2. (a) Time course for the formation of **2** monitored at 360 nm upon addition of $NaNO_2$ (one equiv) to a solution of **4** (1mM) in CH_3CN at 298 K. (b) FT-IR spectrum of **2** recorded in KBr pellet at RT (298 K), showing the peaks for **2**-$^{14}N^{16}O_2^-$ (1270 cm^{-1}) (c) FT-IR spectra of **2**-$^{15}N^{16}O_2^-$ (1244 cm^{-1}) recorded in KBr pellet at RT (298 K) (d) ESI-MS spectrum of **2** recorded in CH_3CN. The peaks at *m/z* *340.1 and 352.1 are assigned to be $[(H_2BPMEN)Cu^{II}Cl]^+$ (calcd: *m/z* 340.1), $[(H_2BPMEN)Cu^{II}(^{15}NO_2^-)]^+$ (calcd: *m/z* 352.1) respectively.

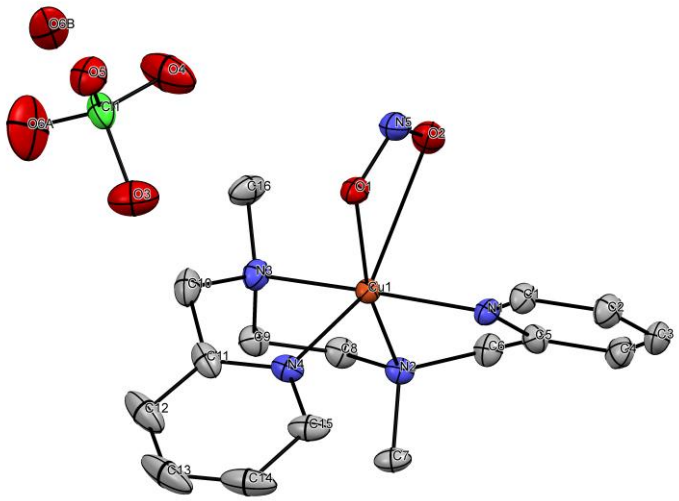

Figure S3. Displacement ellipsoid plots (50% probability level) of **1**. Hydrogen atoms are removed for better clarity.

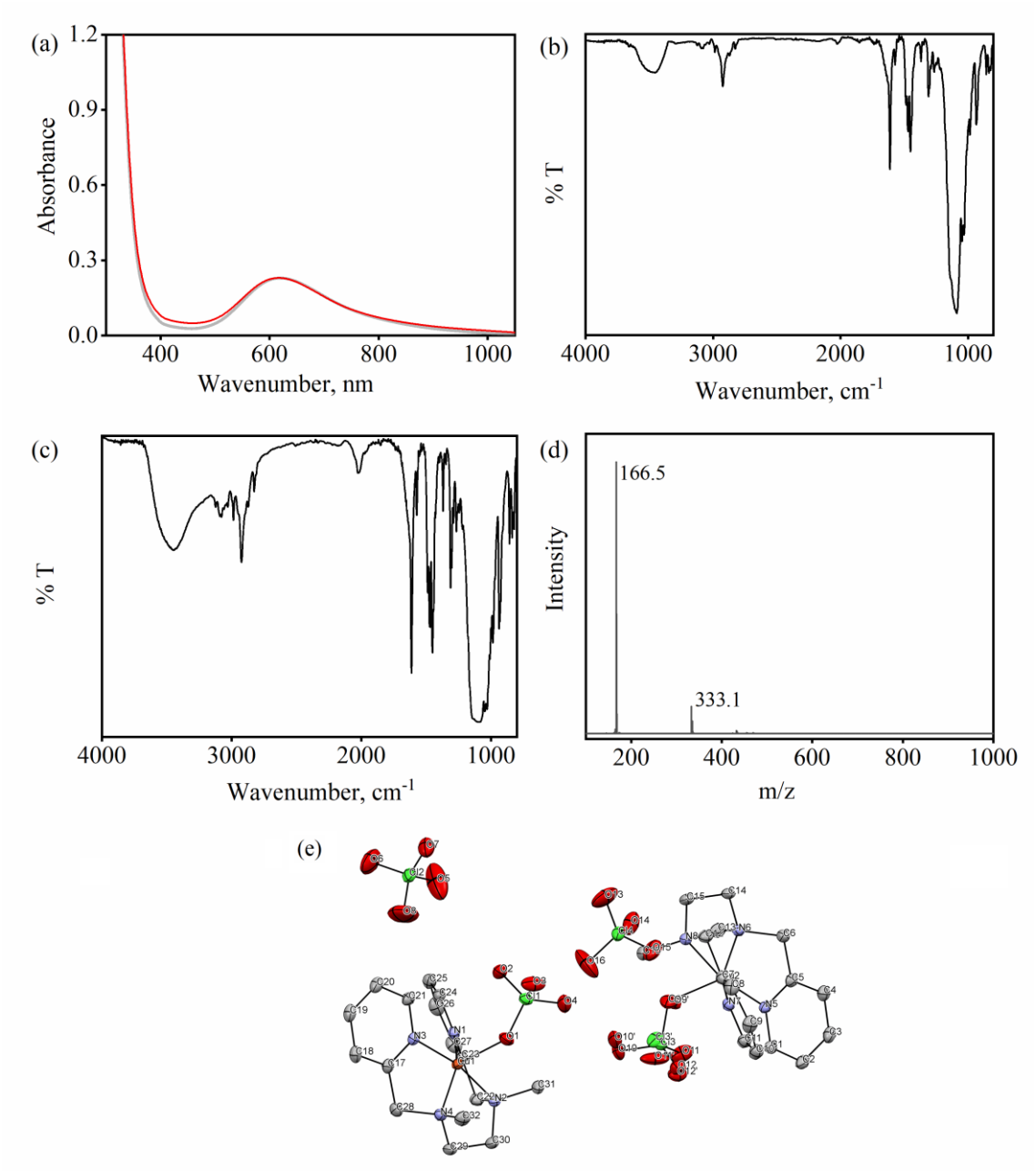

Figure S4. (a) UV visible spectra of the isolated product of the reaction of **1** + one equiv H^+ (Grey line) and authentic **3** (Red line). (b) FT-IR spectrum of the reaction mixture of **1** (1 mM) with one equiv H^+. (c) FT-IR of authentic **3**. (d) ESI-MS spectrum of reaction mixture **1** with one equiv of H^+ in CH_3CN. The peaks at *m/z* 166.5 and 333.1 are assigned to be $[(Me_2BPMEN)Cu^{II}]^{2+}$ (calcd: *m/z* 166.5) and $[(Me_2BPMEN)Cu^{I}]^{+}$ (calcd: *m/z* 333.1), respectively. (e) Displacement ellipsoid plots (50% probability level) of **3.** Hydrogen atoms are removed for better clarity.

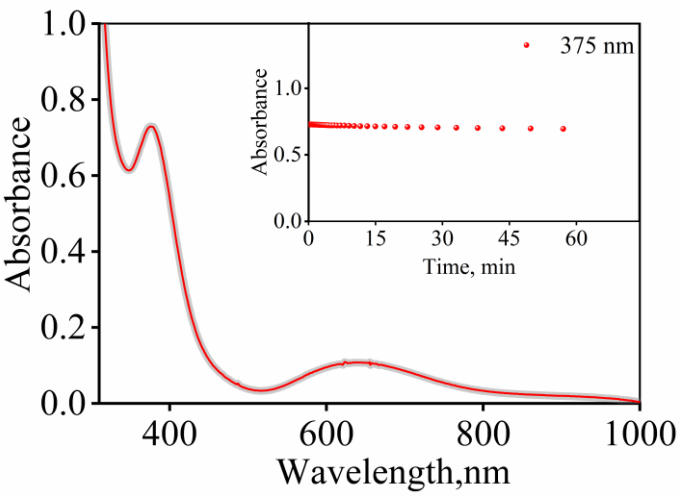

Figure S5. UV-vis spectral changes **1** in CH_3CN at 298 K. The Inset shows a time course natural decay of **1** at 375 nm in CH_3CN at 298 K.

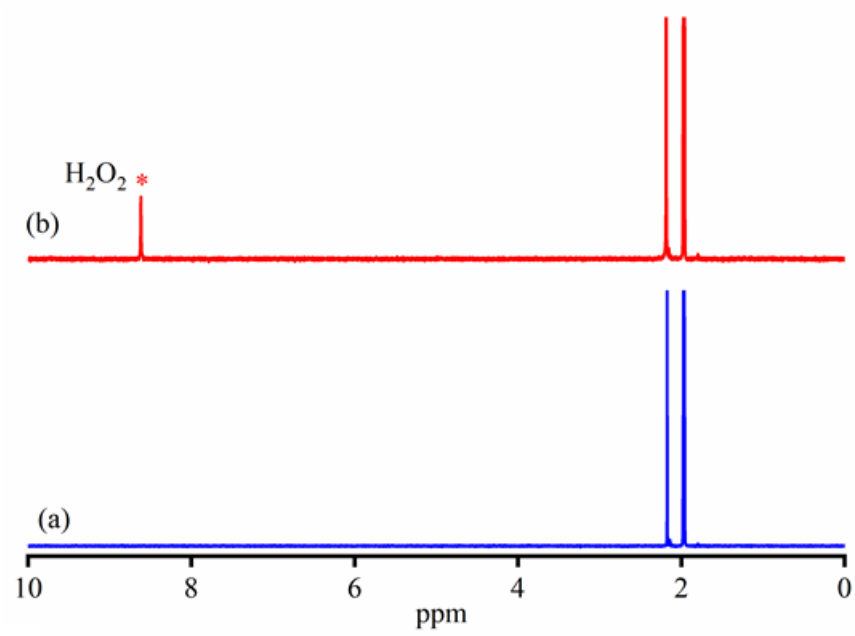

Figure S6. ^{1}H-NMR (400 MHz) spectra of (a) **1** (10 mM) (blue color) (b) reaction of **1** (10 mM) with one equiv of H^{+} recorded just after the addition of H^{+}. The peak of H_2O_2 (red color) was observed at 8.66 ppm in CD_3CN at 298 K.

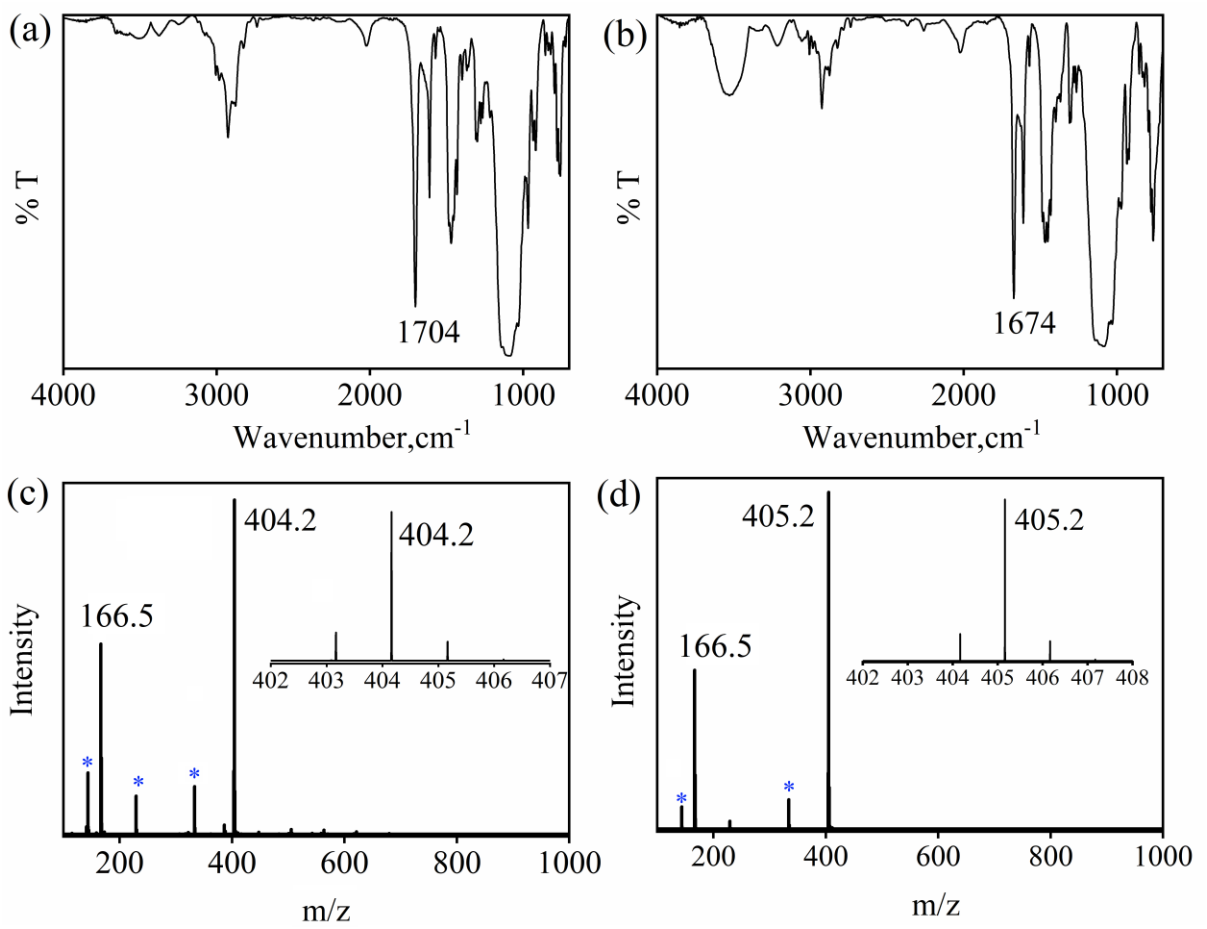

Figure S7. FT-IR spectrum of (a) reaction mixture of **1**-$^{14}NO_2^-$ (40 mM) + $HClO_4$ (one equiv) + [(12-TMC)Co^{II}] $(BF_4)_2$ (one equiv) recorded after completion of the reaction in KBr pellet at 298 K. The spectrum showed a peak for $\{Co^{14}NO\}^8$ (at 1704 cm^{-1}). (b) FT-IR spectrum of the reaction mixture, **1**-$^{15}NO_2^-$ (40 mM) + $HClO_4$ (one equiv) + [(12-TMC)Co^{II}] $(BF_4)_2$ (one equiv), recorded after completion of the reaction in KBr pellet at 298 K. The spectrum showed a peak for $\{Co^{15}NO\}^8$ (at 1674 cm^{-1}). (c) ESI-MS spectrum of **1**-$^{14}NO_2^-$ (40 mM) + $HClO_4$ (one equiv) + [(12-TMC)Co^{II}]$(BF_4)_2$ (one equiv). The peak at m/z 404.2, 166.5 are assigned to be $[(12TMC)Co(^{14}NO)(BF_4)]^+$ and $[(Me_2BPMEN)Cu^{II}]^{2+}$. The asterisk peak at m/z *333.1, *143.6 is assigned as $[(12TMC)Co^{II}(^{14}NO_2^-)]^+$, and $[(12TMC)Co^{II}]^{2+}$. (d) The peak at m/z 405.2, 166.5 are assigned to be $[(12TMC)Co(^{15}NO)(BF_4)]^+$ and $[(Me_2BPMEN)Cu^{II}]^{2+}$. The asterisk peak at m/z *334.1, and *143.6 is assigned as $[(12TMC)Co^{II}(^{15}NO_2^-)]^+$, and $[(12TMC)Co^{II}]^{2+}$.

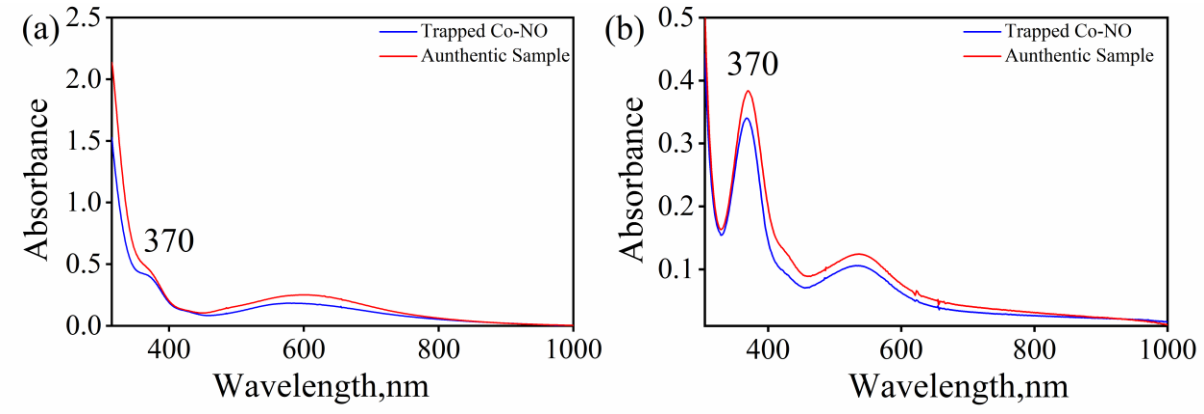

Figure S8. (a) Comparison of UV-Vis spectra of $\{Co\text{-}NO\}^8$ generated in-situ reaction of **1** (0.5 mM) + one equiv H^+ + $[(12\text{-}TMC)Co^{II}(NCCH_3)]^{2+}$ and authentic $[Co(12\text{-}TMC)(NO)]^{2+}$ + **3**. (b) Comparison of UV-Vis spectra of $\{Co\text{-}NO\}^8$ generated by the reaction of **1** (0.5 mM) + one equiv H^+ inside the tube and $[(12\text{-}TMC)Co^{II}(NCCH_3)]^{2+}$ outside tube in closed and degassed culture vials and compared with authentic $[Co(12\text{-}TMC)(NO)]^{2+}$ (0.5 mM). To prepare Figure S8b and compare the UV-Vis spectra, we designed a specific setup (see th figure below) using two sample vials in the Glove box to trap the $NO_{(g)}$ formed in the NO_2^- reduction on Cu^{II}-center of **1**. In this setup, we have kept the CH_3CN solution of **1** in a small sample vial, kept it inside a bigger sample vial containing the CH_3CN solution of $[Co(12\text{-}TMC)(NO)]^{2+}$ (0.5 mM), and closed it with a rubber septum. These samples were prepared in a glove box to avoid the reaction of evolved $NO_{(g)}$ with O_2.

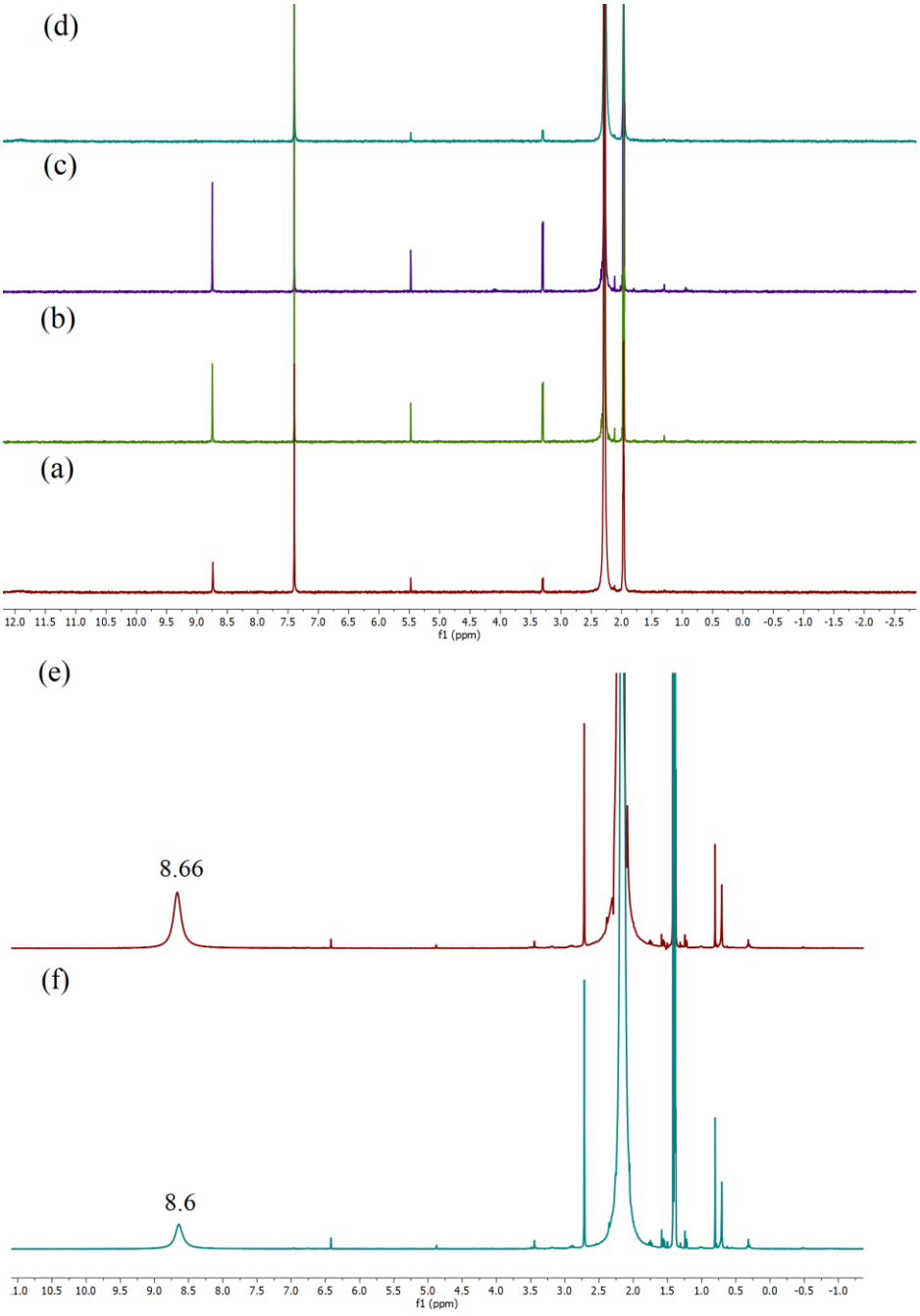

Figure S9. ^{1}H-NMR (400 MHz) spectra of (a) **1** and one equiv H^+ (b) **3** (10 mM) + H_2O_2 (c) H_2O_2 (5 mM) (d) two equiv H^+, using benzene (5 mM) as an internal standard in CD_3CN at RT. (e) H_2O_2 (10 mM) (f) $H_2{}^{18}O_2/H_2{}^{16}O_2$ with one equiv of H^+ in the reaction of **1** (20 mM) and **1-^{18}ONO$^-$** (20 mM) in CD_3CN at 298 K, respectively.

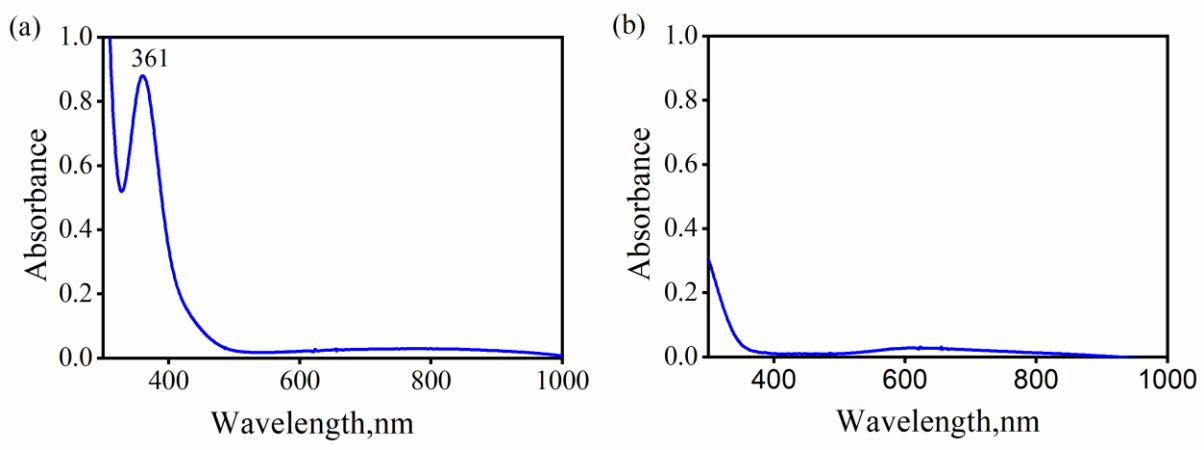

Figure S10. (a) UV-Vis spectra of **1** (0.1 mM) with one equiv of H^+ followed by the addition of 1.5 equiv of NaI recorded in CH_3CN at 298 K. Peak observed at 361 nm corresponds to I_3^-. (b) UV-Vis spectra of **1** (0.1 mM) with two equiv of H^+ followed by adding one equiv of NaI were recorded in CH_3CN at 298 K; no peak at 361 was observed.

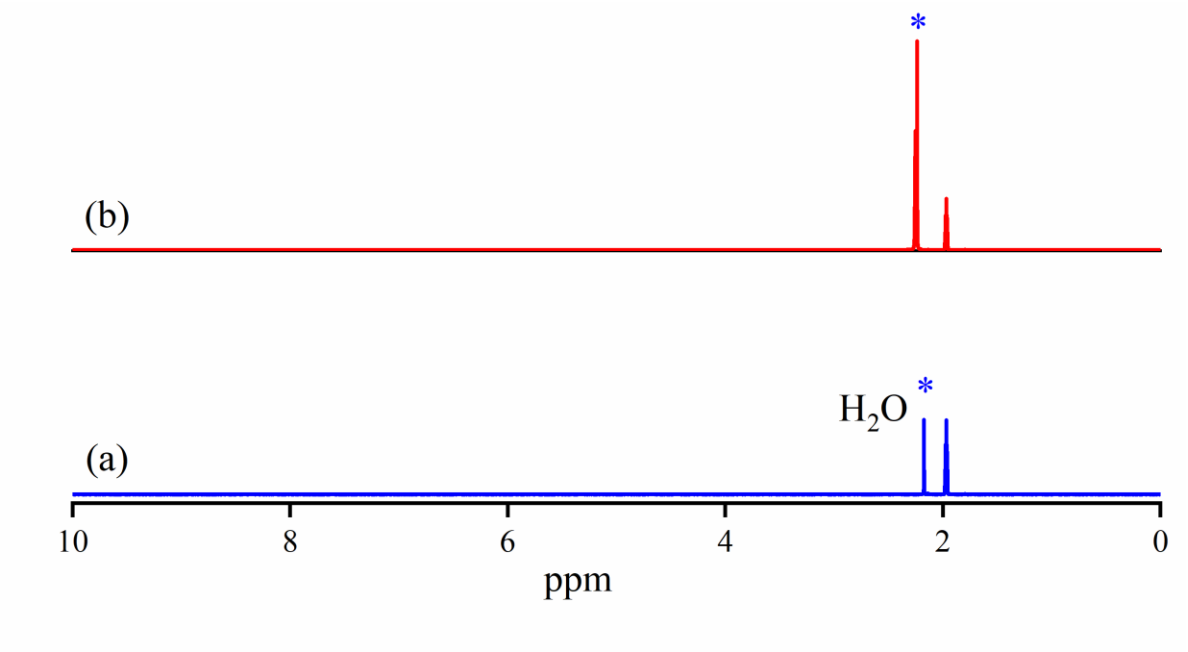

Figure S11. ^{1}H-NMR (400 MHz) spectra of (a) **1** (10 mM) (b) reaction of **1** (10 mM) with two equiv of H^{+}. The peak of H_2O (red color) was observed at 2.2 ppm in CD_3CN at 298 K.

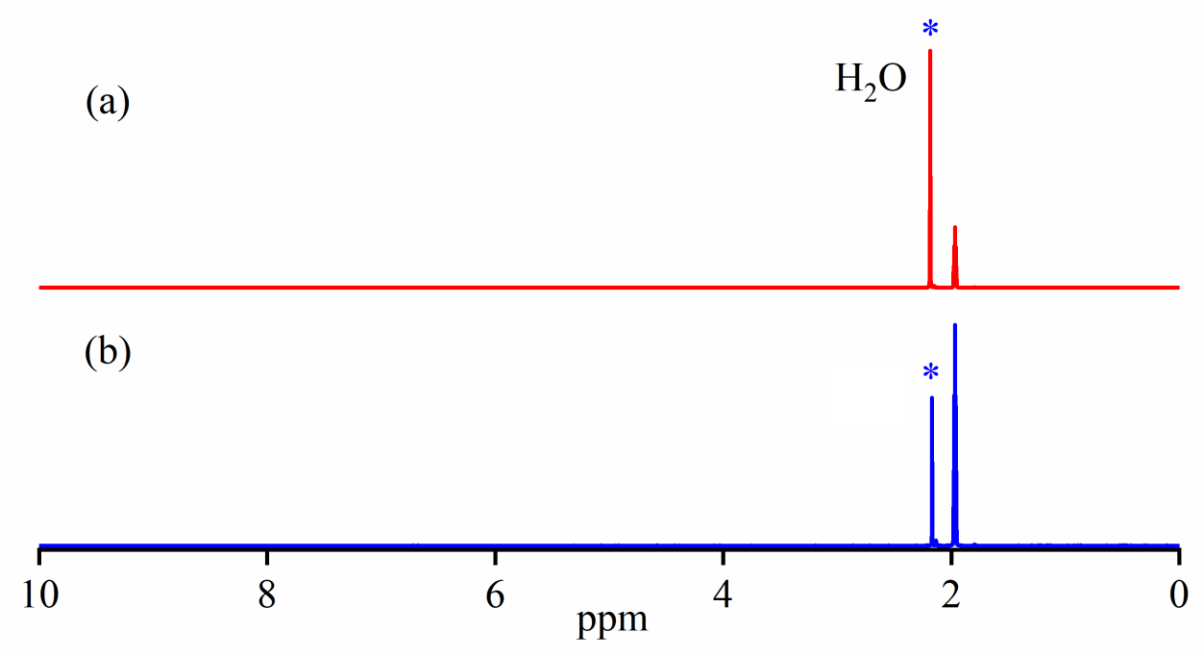

Figure S12. ^{1}H-NMR (400 MHz) spectra of (a) **1** (10 mM) with two equiv of H^{+}. A peak of H_2O (red color) was observed at 2.2 ppm (b) reaction of **1** (10 mM) with two equiv of D^{+} (blue color) in CD_3CN at 298 K.

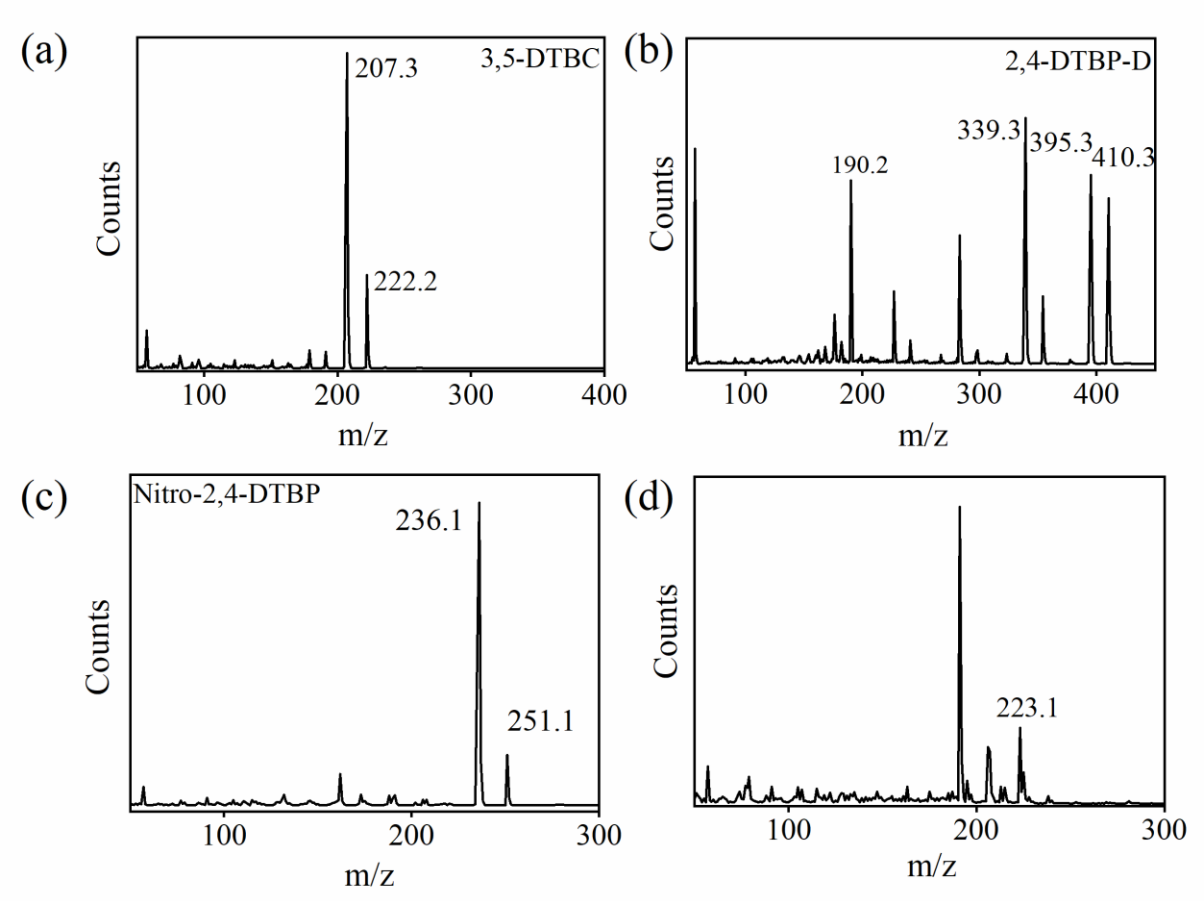

Figure S13. GC-MS characterization of product formed in the reaction of **1** with 2,4-DTBP and one equiv H^+ (a) 3,5-Di-*tert*-butylcatechol (3,5-DTBC); The peak at *m/z* value 222.2, 207.3 are assigned to 3,5-DTBC and CH_3 loss from 3,5-DTBC, respectively. (b) 2,4-DTBP-dimer (2,4-DTBP-D); The peaks at *m/z* 410.3, 395.3, 339.3, and 190.2 are assigned to be 2,4-DTBP-D, loss of CH_3 from 2,4-DTBP-D, loss of C_4H_8 and CH_3 from 2,4-DTBP-D and loss of CH_3 from monomer 2,4-DTBP. (c) nitro-2,4-DTBP (nitro-2,4-DTBP): The peaks at *m/z* 251.2 and 236.2 are assigned to be nitro-2,4-DTBP and loss of CH_3 from nitro-2,4-DTBP. (d) The reaction of **1** with 2,4-DTBP and one equiv of $DClO_4$ (source of D^+). The peak at 223.1 corresponds to 3,5-DTBC-OD. The peaks were compared with the NIST standard library.

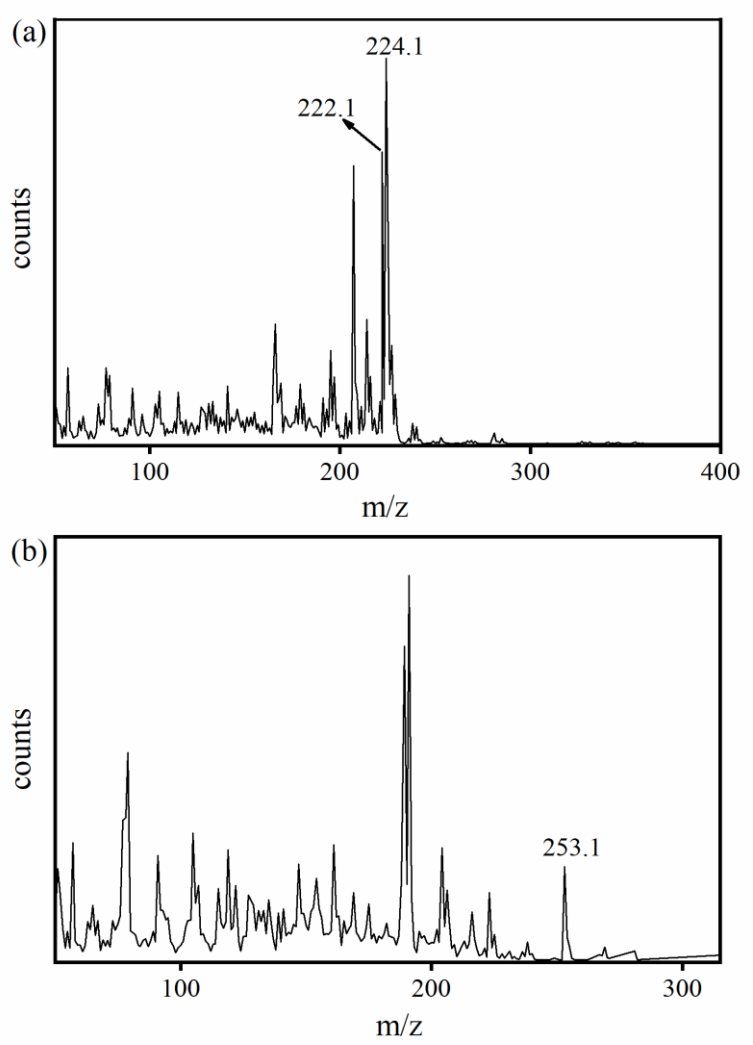

Figure S14. GC-MS characterization of product formed in the reaction of **1-^{18}ONO^{-}** with 2,4-DTBP and one equiv H^{+} (a) 3,5-DTBC-^{18}OH^{16}OH (calc. = 224.1) and 3,5-DTBC-^{16}OH^{16}OH (222.1). (b) The peaks at *m/z* 253.1 correspond to nitro-2,4-DTBP (^{16}O^{14}N^{18}O-2,4-DTBP).

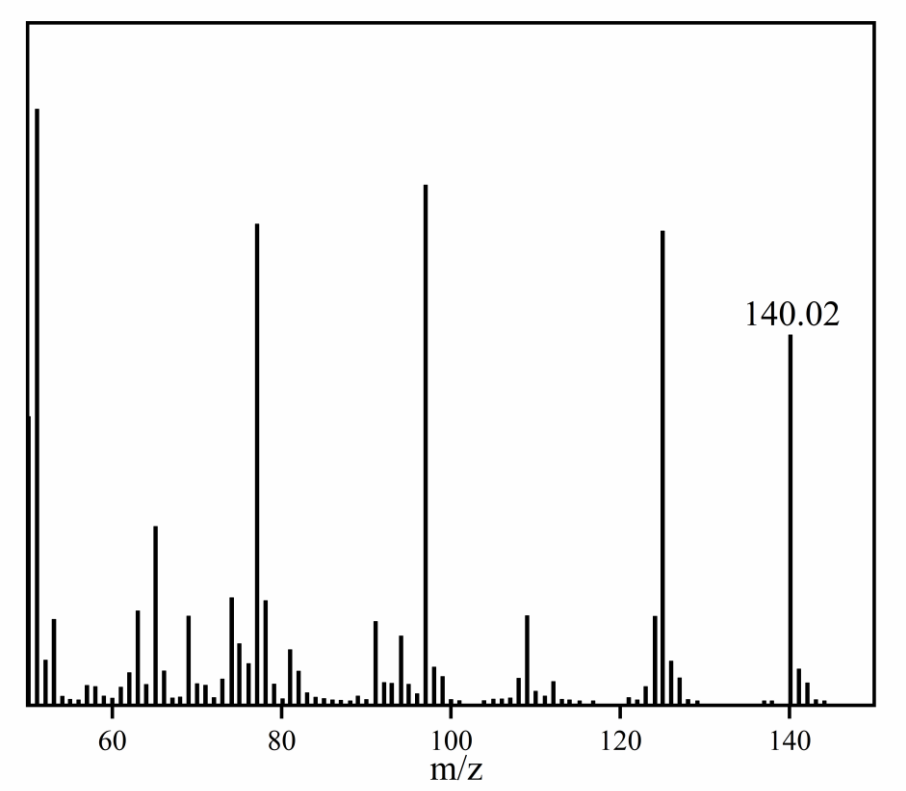

Figure S15. GC-MS characterization of product formed in the reaction of **1** with thioanisole and one equiv H^+ showing formation on methyl phenyl sulfoxide (calc. = 140.02).

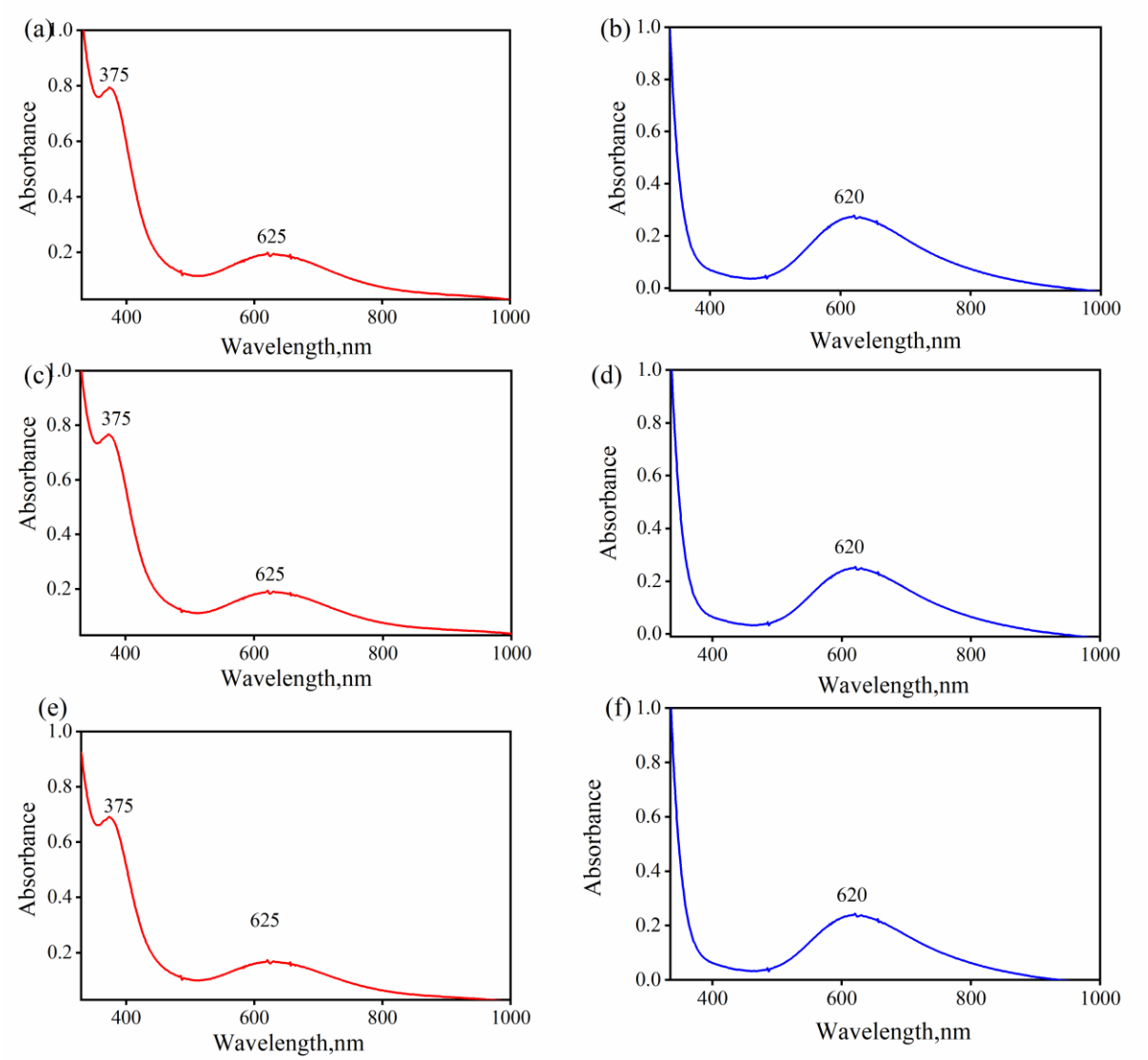

Figure S16. (a) UV-Vis spectrum of **1** (1 mM) (Red line). (b) UV-Vis spectrum of **3** (1 mM) isolated from the reaction of **1** + one equiv H^+ (blue line) after the first cycle. (c) UV-Vis spectrum of **1** obtained after adding $NaNO_2$ to **3** generated after the first cycle of reaction of **1** (1 mM) + one equiv H^+ (red line) (d) UV-Vis spectrum of **3** obtained after carrying out five cycles of reaction of **1** with one equiv H^+ followed by addition of $NaNO_2$ then H^+ (blue line). (e) UV-Vis spectrum of **1** obtained after adding $NaNO_2$ to **3** generated after the ten cycles of reaction of **1** + one equiv H^+ followed by $NaNO_2$ then H^+ (red line) (f) UV-Vis spectrum of **3** obtained after carrying out ten cycles of reaction of **1** with one equiv H^+ followed by addition of $NaNO_2$ then H^+ (blue line).

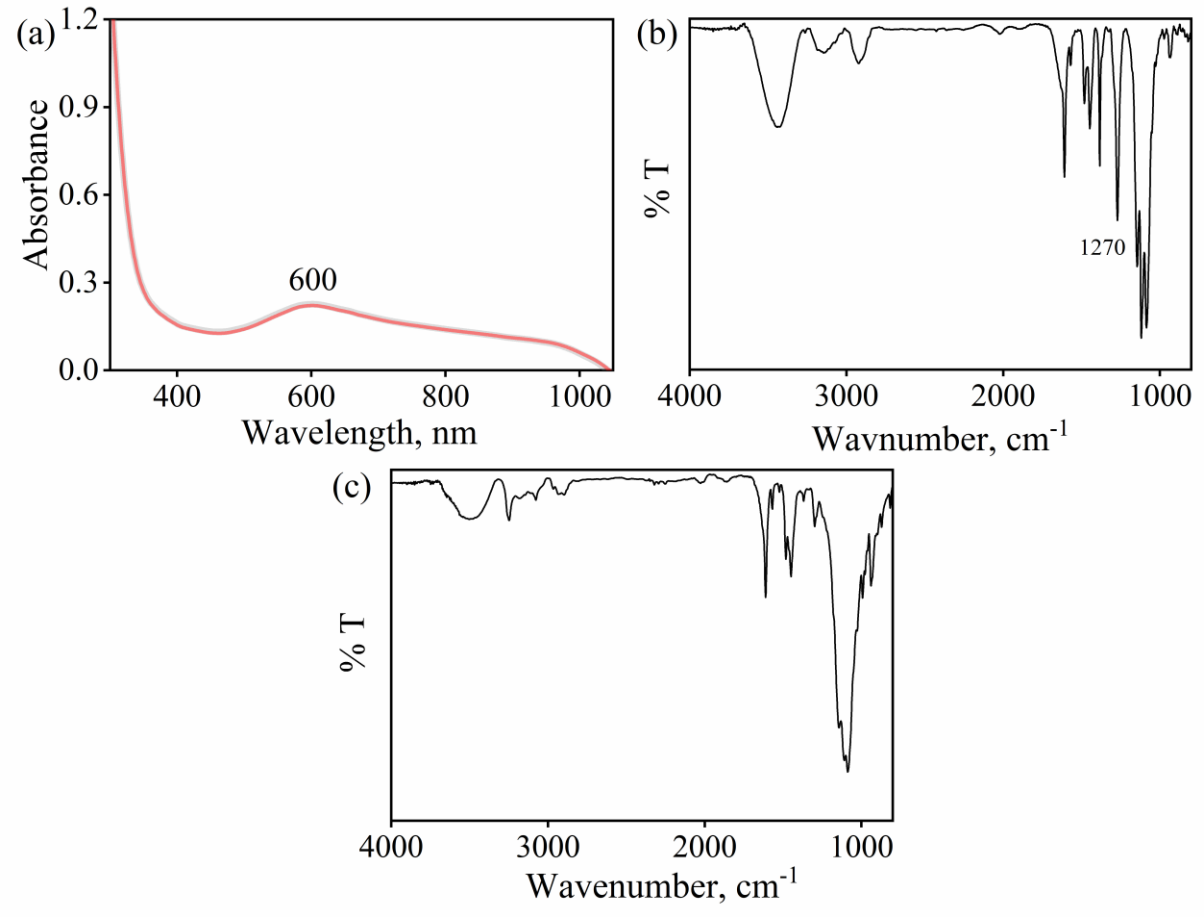

Figure S17. (a) UV-Vis spectra of the isolated product of the reaction of **2** + one equiv H^+ (Grey line) and authentic **4** (Red line) (b) FT-IR spectra (KBr palette) of **2**, and (c) FT-IR spectra (KBr palette) of **4** obtained in the reaction of **2** and one equiv of H^+.

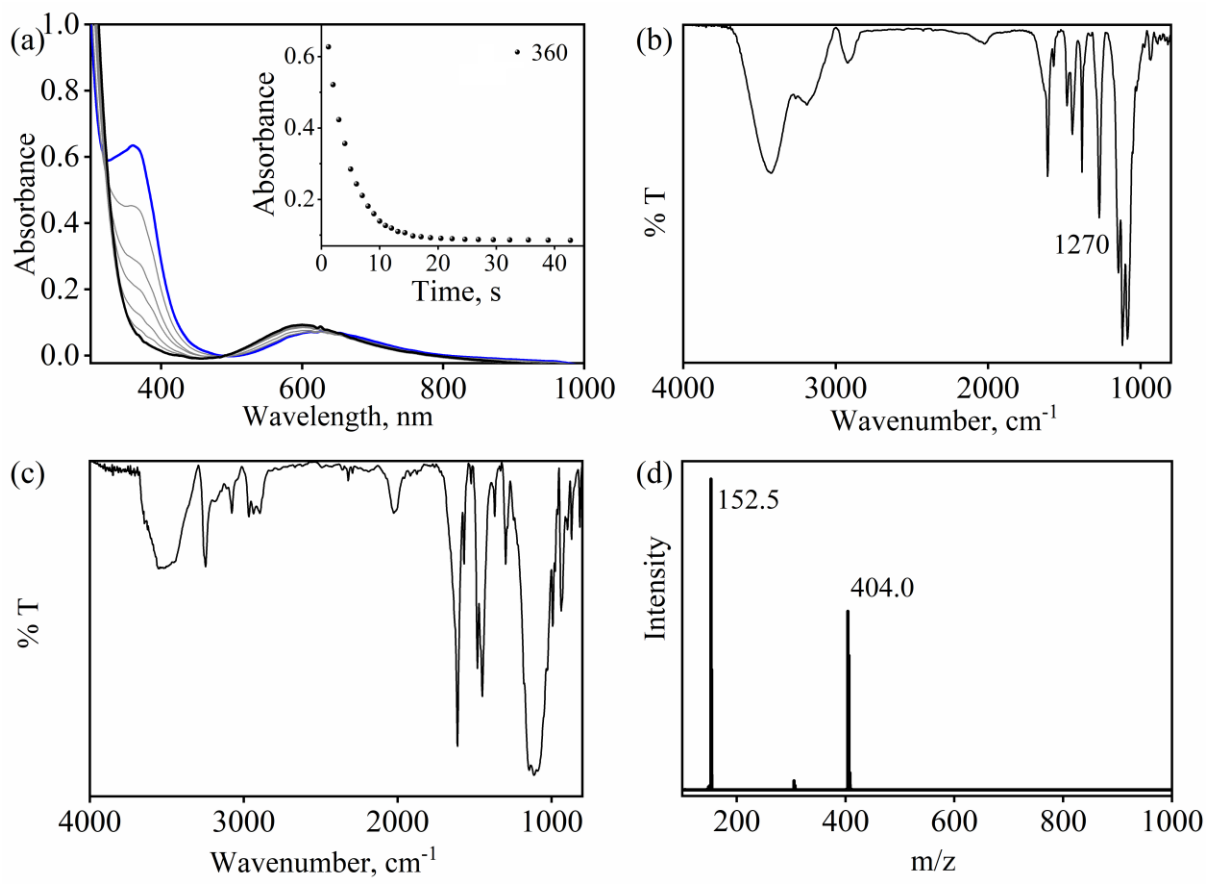

Figure S18. (a) UV-Vis spectra of **2** (1 mM) with two equiv of H^+. Inset shows the time course decay of **2** (black circles) monitored at 360 nm upon addition H^+ (two equiv) to a solution of **2** (1 mM) in CH_3CN at 298 K (b) FT-IR spectra (KBr palette) of **2** (c) FT-IR spectra (KBr palette) of **4** obtained in the reaction of **2** and two equiv of H^+ (d) ESI-Ms spectra of **4** obtained in the reaction of **2** and two equiv of H^+; The peaks at *m/z* 152.5, and 404.0 are assigned to be $[(2PYENH_2)Cu^{II}]^{2+}$ (calcd: *m/z* 152.5), and $[(2PYENH_2)Cu^{II}(ClO_4]^+$ (calcd: *m/z* 404.0), respectively.

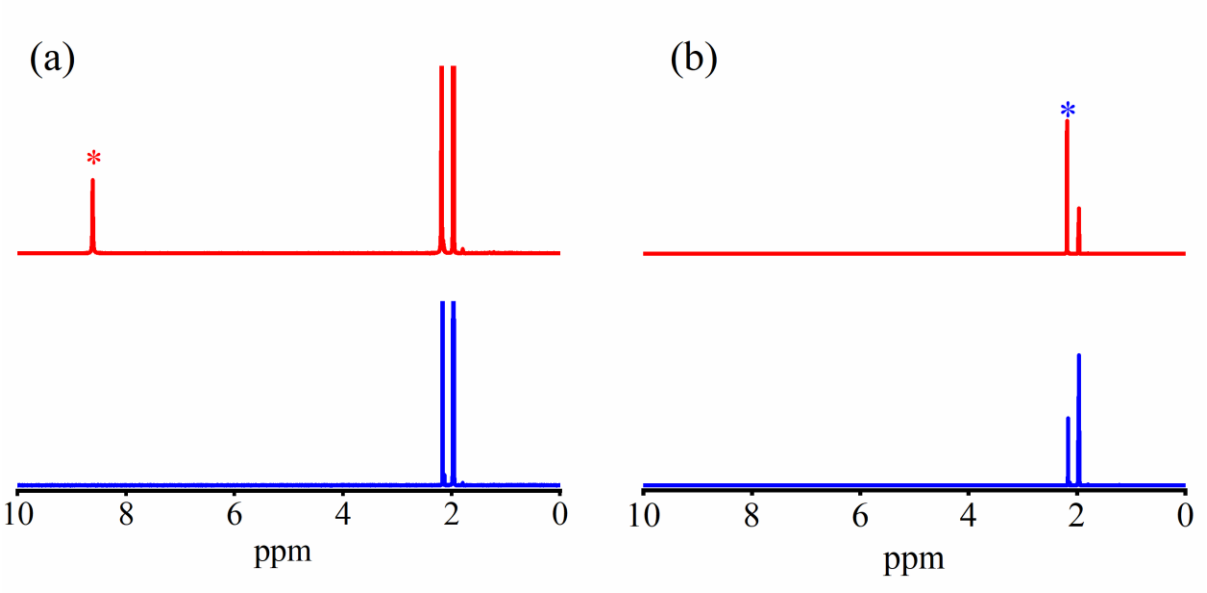

Figure S19. ^{1}H-NMR (400 MHz) spectra of (a) **2** (10 mM) with one equiv of H^{+}. A peak of H_2O_2 (red color) was observed at 8.66 ppm in CD_3CN at 298 K. (b) reaction of **2** (10 mM) with two equiv of H^{+}. The peak of H_2O (red color) was observed at 2.2 ppm in CD_3CN at 298 K.

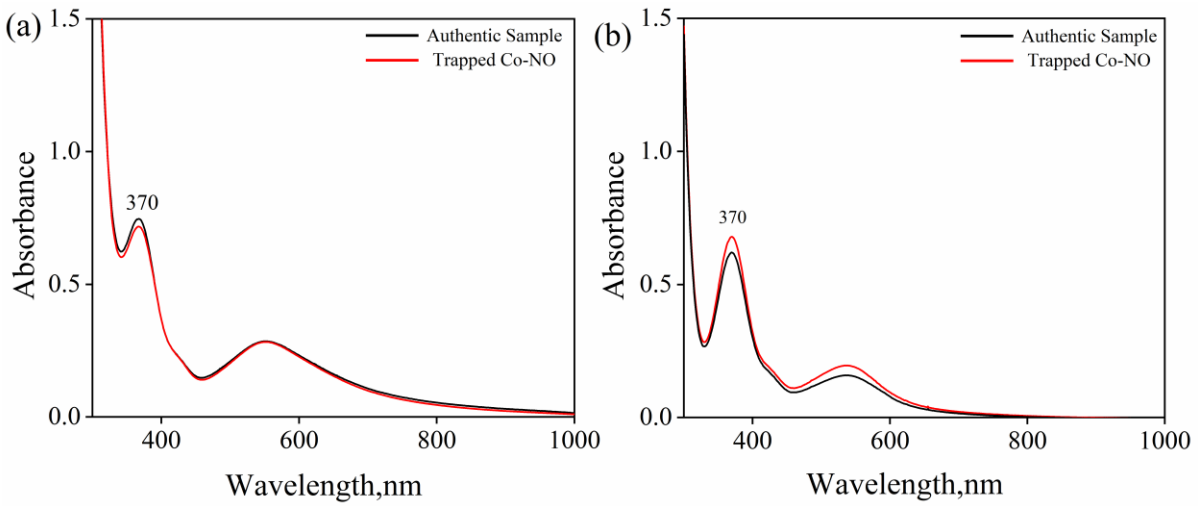

Figure S20. (a) UV-Vis spectra of **2** (1 mM) with one equiv of H^+ and one equiv of [(12-TMC)$Co^{II}(CH_3CN)]^{2+}$ (1 mM) (red color) comparing it with authentic, $\{CoNO\}^8$ (1 mM) + **4** (1 mM) (black color). (b) Comparison of UV-Vis spectra of trapped $\{CoNO\}^8$ generated by reaction of **2** (1mM) + one equiv H^+ inside tube and [(12-TMC)$Co^{II}(NCCH_3)]^{2+}$ outside tube in closed and degassed culture vials and compared with authentic $\{CoNO\}^8$.

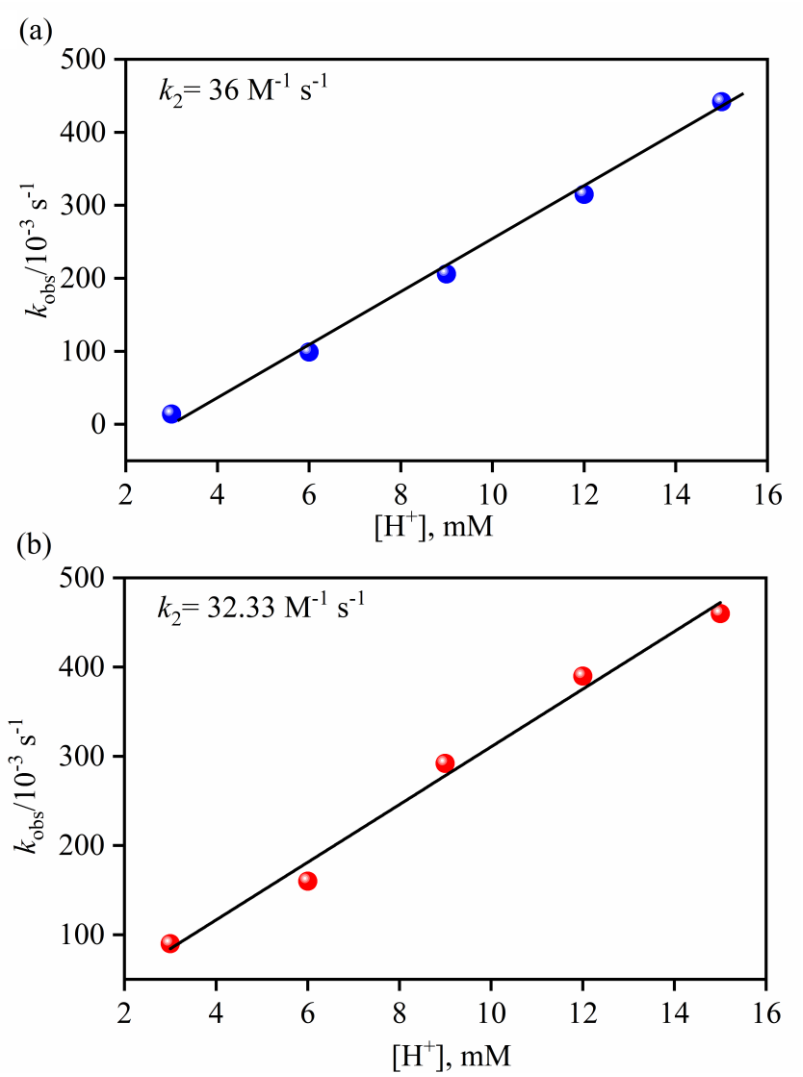

Figure S21. Plots of pseudo-first-order rate constant (k_{obs}) for the formation of (a) **3** and (b) **4** against the concentration of H^+ to determine the second-order rate constant (k_2) in the reaction of (a) **1** and (b) **2** with H^+.

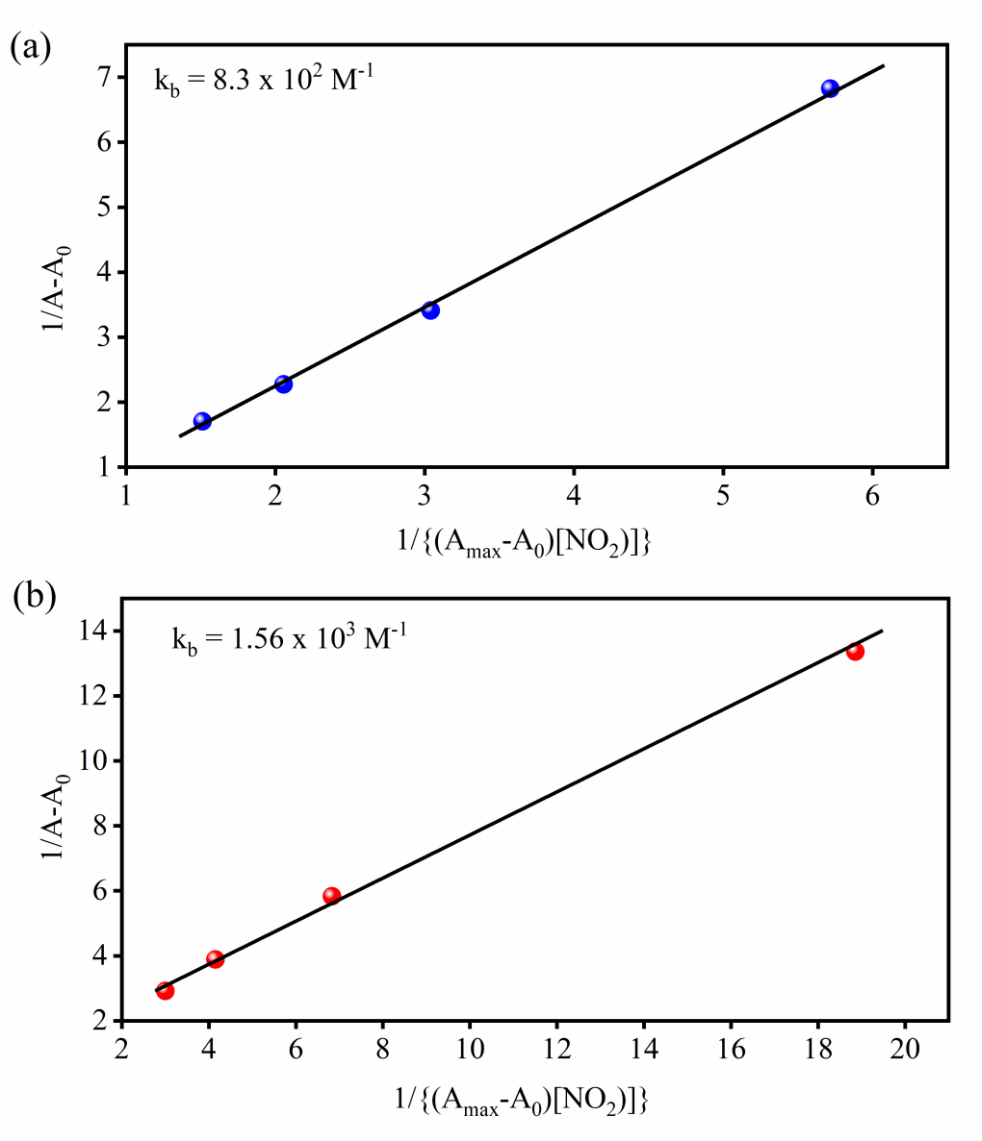

Figure S22. Binding Constant of (a) **3** and (b) **4** with NO_2^-; calculated from the Benesi-Hildebrand equation.

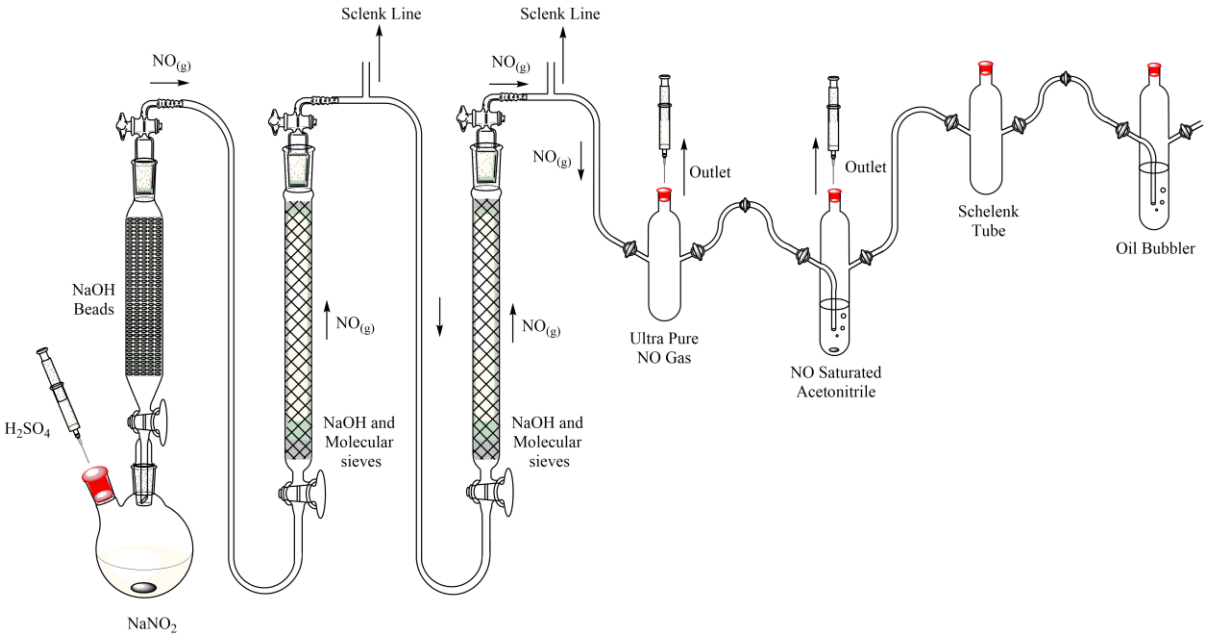

Figure S23. Schematic diagram showing the generation and purification setup for NO.